Mon. Not. R. Astron. Soc. **000**, 000–000 (0000) Printed 26 November 2008 (MN LATEX style file v2.2)

Early evolution of newly born magnetars with a strong toroidal field

S. Dall'Osso[1,2], S. N. Shore[1] and L. Stella[2]
[1] *Università degli Studi di Pisa, Dipartimento di Fisica "E. Fermi" & INFN, Largo B. Pontecorvo 3, Pisa, Italy*
[2] *INAF - Osservatorio Astronomico di Roma, via di Frascati 33, 00040 Monteporzio Catone (Roma)*

November 20 2008

ABSTRACT
We present a state-of-the-art scenario for newly born magnetars as strong sources of Gravitational Waves (GWs)in the early days after formation. We address several aspects of the astrophysics of rapidly rotating, ultramagnetized neutron stars (NSs), including early cooling before transition to superfluidity, the effects of the magnetic field on the equilibrium shape of NSs, the internal dynamical state of a fully degenerate, oblique rotator and the strength of the electromagnetic torque on the newly born NS. We show that our scenario is consistent with recent studies of SNRs surrounding AXPs and SGRs in the Galaxy that constrain the electromagnetic energy input from the central NS to be $\leqslant 10^{51}$ erg (Vink & Kuiper 2006). We further show that if this condition is met, then the GW signal from such sources is potentially detectable with the forthcoming generation of GW detectors up to Virgo cluster distances where an event rate ~ 1/yr can be estimated (Stella et al. 2005). Finally, we point out that the decay of an internal magnetic field in the 10^{16} G range couples strongly to the NS cooling at very early stages, thus significantly slowing down both processes: the field can remain this strong for at least 10^3 yrs, during which the core temperature stays higher than several $\times 10^8$ K.

Key words: – – –

1 INTRODUCTION

Gravitational wave emission from spheroidal, rapidly rotating, isolated NSs has long been considered in the astrophysical literature (Ostriker & Gunn 1969). A natural origin of this distortion can be the anisotropic pressure from the internal magnetic field. However, before the early nineties, the inferred magnetic fields of NSs were $\sim 10^{13}$ G, which implied tiny deviations from spherical symmetry and, thus, weak GW emission that would be detectable, in principle, only from the nearest sources and with years-long observations (Bonazzola & Gourgoulhon 1996).
The discovery of the Soft Gamma Ray Repeaters (SGRs) and Anomalous X-ray Pulsars (AXPs) (cfr. Mazets et al. 1979, Mereghetti & Stella 1995) led to the idea that these peculiar high-energy sources could be ultramagnetized NSs, magnetars, with external (dipole) fields in the $10^{14} \div 10^{15}$ G range and with internal fields at least one order of magnitude stronger (Paczynsky 1992, Duncan & Thompson 1992, DT92 hereafter, Thompson & Duncan 1993, 1995, 1996, hereafter TD93; TD95; TD96, respectively). The core of the proto-neutron star (PNS) experiences a phase of neutrino-driven turbulent convection (during a few tens of seconds). Strong differential rotation is also present if the nascent NS is spinning at millisecond period (we indicate the initial spin, in milliseconds, as P_i/ms), providing a total free energy reservoir of up to $\sim 10^{52}(P_i/\mathrm{ms})^{-2}$ erg. The combination of these two factors can power an $\alpha - \Omega$ dynamo that acts coherently over the whole NS core (DT92). A seed magnetic field is twisted into a mainly toroidal configuration and its intensity amplified to values $\sim 10^{16}$ G. The total energy available from the core differential rotation corresponds to a maximum field of $\sim 10^{17}$ G (TD93; Duncan 1998). Millisecond spin periods are required for differential rotation to play an important role and to achieve magnetic field coherence lengthscales comparable to the stellar radius. In more slowly rotating NSs differential rotation is almost negligible and a convection-driven, α-type dynamo results that acts stochastically and leads to a much weaker large scale field (DT92; TD93). In this formation scenario, magnetars represent those NSs that are born very rapidly rotating, at $\leqslant 3$ ms spin period.
As the magnetar model received increasing support from observations during the last decade it was shortly after realized that such objects at birth represent promising sources of GWs, because of their large magnetic deformation and rapid rotation (Ioka 2001; Palomba 2001). These early suggestions assumed that a simple dipole field extended throughout the NS and its magnetosphere thus causing NS deformation and

magnetodipole spindown. Cutler (2002) first highlighted the crucial role of the internal field structure in the GW emission efficiency of a magnetically distorted NS. He pointed out that a NS with a strong internal toroidal field has a prolate shape and would thus provide the best chance of being a strong GW emitter. Conversely, GW emission from a NS with an oblate distortion (such as that caused by a dipole field) would be rapidly quenched, since such an object would tend to spin around its symmetry axis (see § 2). Based on the energetics and likely recurrence time of Giant Flares such as the Dec 27 event from SGR 1806-20, Stella et al. (2005) derived a lower limit of $\sim 8 \times 10^{15}$ G for the strength of the core magnetic field in this object. This suggests that internal fields of magnetars may be even stronger than previously thought, reaching the 10^{16} G range. Lazzati et al. (2005), Nakar et al. (2006) and Popov & Stern (2006), based on the apparent lack of Giant Flare-like events in the BATSE archive, suggest longer recurrence times for such events, thus reducing the minimum energy requirement proposed by Stella et al. (2005). However, the correlation between short GRBs and local galaxies found by Tanvir et al. (2005) leaves room for a fraction of such events to be associated with a population of young NSs. Furthermore, Kaminker et al. (2007) showed that, if the thermal emission observed from AXPs is indeed powered by the decay of a magnetar's B-field, then the field strength in the NS crust must be $\sim 10^{16}$ G.

Fields $\sim 10^{16}$ G would imply remarkably large (prolate) magnetic deformations, $\epsilon_B \sim 10^{-3}$ (see § 2.1.2) which, in turn, would make GW emission at birth from such objects strong enough to be detectable up to the Virgo cluster distance, with Advanced LIGO/Virgo-class detectors. The integrated magnetar formation rate in Virgo is estimated to be ~ 1 per year (Stella et al. 2005), as opposed to $\sim 10^{-3}$ per year in the Galaxy alone (Gaensler et al. 1999), thus making newly formed magnetars potentially interesting sources for next generation GW detectors, with a fairly high rate of occurence.

As an alternative scenario, it was proposed that strongly magnetic NSs can form as a direct result of magnetic flux conservation during core-collapse of a massive star with unusually strong magnetic field (Ferrario & Wickramasinghe 2006, cf. Usov 1992). In this picture, magnetars need not be born rapidly rotating: their magnetic field is stronger than in ordinary NSs because the magnetic dipole moment of their progenitor stars was particularly large. Ferrario & Wickramasinghe (2006) have shown that a population of NSs with dipole fields up to $\sim 10^{15}$ G can be obtained in this framework starting from a realistic Galactic population of high-mass, high-field stars. We note, however, that the upper end of their field distribution seems to fall short of the minimal requirement within the magnetar model. Internal fields of *at least* several times 10^{15} G are needed both to explain the overall energy output of SGRs and AXPs (TD95, Thompson & Duncan 2001, hereafter TD01), and to make the magnetic field decay timescale comparable to, or shorter than, the estimated ages ($\sim 10^4$ yrs) of these sources (TD96).

Geppert & Rheinhardt (2006) have shown that a field amplified to magnetar-strength in a newly formed NS will survive an early unstable phase (and subsequent dissipation) only if the NS spin period is shorter than ~ 5 ms, thus reinforcing the case for fast spins at birth.

If magnetars are born with millisecond spin periods (hereafter millisecond magnetar), their initial spin energy will be $E_{\rm spin} \sim 3 \times 10^{52} ({\rm P_i/ms})^{-2}$ erg. Here and throughout we assume a typical radius of 12 km and a mass of 1.4 $M_\odot$. The spindown timescale through magnetic dipole radiation will be very short, $\sim$ one day for external dipole fields in the 10^{14} G range. Most of the initial spin energy would thus be rapidly transferred to the surrounding supernova ejecta (Allen & Horvath 2004). Recent studies have also shown that, for newly formed magnetars with dipole fields in excess of $\sim (6 \div 7) \times 10^{14}$ G and spin period of $\approx$ 1 ms, strongly magnetized, relativistic winds are produced which can carry away most of the initial spin energy in a matter of minutes, thus opening the possibility of an even faster transfer of energy to the ejecta (Thompson et al. 2004; Bucciantini et al. 2006; Metzger et al. 2007). In both cases, present-day SNRs around known magnetars should bear the signature of this larger-than-usual energy injection. For initial spin periods less than 3 ms, the injected energy would be $> 3 \times 10^{51}$ erg, making these remnants significantly more energetic than those surrounding ordinary NSs.

The X-ray spectra of the SNRs surrounding known magnetar candidates (two APXs and two SGRs) have been analyzed by Vink & Kuiper (2006) who found that the total energy content of the ejecta in these remnants does not appear to be different from the energy in remnants surrounding common NSs ($\approx 10^{51}$ erg). This result implies that either these NSs were not born rapidly rotating, thus challenging the $\alpha - \Omega$ dynamo scenario, or their initial spin energy must have been lost without appreciably energizing the surrounding ejecta. Dall'Osso & Stella (2007) discussed the possibility that most of the initial spin energy of millisecond magnetars is realeased through gravitational radiation. They concluded that, in order to account for the constraints derived by Vink & Kuiper (2006), the internal toroidal field at birth should be in the 10^{16} G range, consistent with the inference by Stella et al. (2005) for the field strength in SGR 1806-20 and, by extension, magnetars in general. A similar conclusion about strong GW-driven spindown in newly formed magnetars was reached by Arons (2003), based on a totally independent argument.

Bucciantini et al. (2007) have also studied the possibility that the huge spin energy of a millisecond magnetar is promptly released in the form of a highly collimated wind, if the external (dipole) field exceeds 10^{15} G. The wind breaks through the surrounding supernova ejecta and produces a GRB-like event without directly energizing the ejecta. However, the currently estimated magnetar formation rate exceeds the rate of observed GRBs by 2 orders of magnitude. Hence, this process can involve at most a tiny fraction of newly formed magnetars (Bucciantini et al. 2007).

Thus, a number of astrophysical arguments point to possible field strengths in the 10^{16} G range in magnetar interiors and suggest a possibly relevant role of GW emission in the early evolution of these objects. The aim of this paper is to explore the physical consequences of this hypothesis and draw a state-of-the-art scenario, in light of all approximations and uncertainties. The paper is organised as follows: in § 2 we introduce the model for the early spindown of a magnetar subject to both magnetodipole and GW torques and study the main factors determining the GW emission

efficiency of a newly formed magnetar. In § 3 we calculate the expected energy loss through GW emission from newly born magnetars as a function of the relevant NS parameters and re-address the problem of signal detection already discussed by Stella et al. (2005). Finally, in § 5 we address the problem of the thermal and magnetic evolution of NSs, extending previous treatments of field decay to field strengths $\sim 10^{16}$ G.

2 MAGNETAR EARLY SPINDOWN: ELECTROMAGNETIC VS. GW EMISSION

A newly formed NS with a strong toroidal magnetic field has a prolate deformation induced by the field (ϵ_B, defined in § 2.1.2) with symmetry axis along the magnetic axis. If the magnetic and spin axes are misaligned, with tilt angle χ, the angular velocity vector ($\mathbf{\Omega}$) precesses (in the NS frame) around the fixed angular momentum vector ($\boldsymbol{L}$). Cutler & Jones (2001) (see also Cutler 2002) studied the precession dynamics taking also into account the effects of the centrifugal deformation of the NS. They showed that the triaxial ellipsoid behaviour is, in this case, formally equivalent to that of a biaxial rigid body, as far as the precessional motion is concerned. If I_0 represents the moment of inertia of the spherical NS, the eigenvalues for the distorted NS are $I_1 = I_2 = I_0 - (1/3)\Delta I_\Omega - (1/3)\Delta I_B$ and $I_3 = I_1 + \Delta I_B$, where ΔI_Ω represents the centrifugal deformation. Since the latter term affects all eigenvalues in the same way it does not enter explicitly in the precession dynamics, which are determined only by the magnetic deformation (see Appendix A). Hence, the focus here and in the following will be on the magnetic deformation only.

The spin energy of a rotating spheroid is minimized, at fixed angular momentum, when its moment of inertia is maximum. For a prolate figure, this is achieved when the symmetry axis is orthogonal to the spin axis. In the presence of internal dissipative processes, the magnetic axis of a prolate NS will thus be driven towards orthogonal rotation (Mestel & Takhar 1972; Jones 1976), which maximizes the efficiency of GW emission[1] (Cutler 2002).

For arbitrary χ, GWs will be emitted at both the spin frequency and its octave, with a total rate of energy emission (cfr. Cutler & Jones 2001 and references therein)

$$\dot{\mathrm{E}}_{\mathrm{gw}} = -\frac{2}{5}\frac{G(\mathrm{I}\epsilon_B)^2}{\mathrm{c}^5}\ \omega^6\ \sin^2\chi(1+15\sin^2\chi) \qquad (1)$$

An orthogonal rotator emits GWs only at twice its spin frequency, at the rate given by eq. (1) with $\chi = \pi/2$

$$\dot{\mathrm{E}}_{\mathrm{gw}}(\chi=\pi/2) = -\frac{32}{5}\frac{G(\mathrm{I}\epsilon_B)^2}{c^5}\ \omega^6 \qquad (2)$$

Given the generation mechanism for the superstrong internal field, the magnetic axis is expected to be just slightly tilted, initially, to the spin axis and, for small χ, the GW luminosity is largely suppressed (eq. 1). Given the efficiency of magnetodipole radiation at birth, the orthogonalization process must thus be quick enough for strong GW emission to ensue promptly, in order to be competitive with magnetodipole radiation.

Strictly speaking, the spindown luminosity of a magnetic dipole rotating in vacuo depends only on the magnitude of the dipole component orthogonal to the spin axis. However, according to the standard pulsar model, an aligned rotator is expected to have a spindown luminosity comparable to that of an orthogonal rotator. Studies on the structure of force-free NS magnetospheres suggest that this is indeed the case, within a factor of order unity (Contopoulos, Kazanas & Fendt 1999; Gruzinov 2006; Spitkovsky 2006). Based on these results, we assume a newly formed magnetar to have the magnetodipole luminosity of an orthogonal rotator. Further discussion of these issues is delayed to § 4.

We neglect here the effects of strongly magnetised winds from newly formed magnetars spinning at ≈ 1 ms period and restrict our attention to external dipole fields $\leqslant 5\times10^{14}$ G. Although such winds can be extremely efficient in carrying away angular momentum (and spin energy) from the NS in just a few minutes, their efficiency is expected to be negligible for dipole fields weaker than $(6 \div 7)\times10^{14}$ G (Thompson et al. 2004; Bucciantini et al. 2006; Metzger et al. 2007).

To summarize, we describe the early spin evolution of a newly born magnetar as being driven by both magnetodipole and GW torques. Hence, as the tilt angle χ increases, a sufficiently large (prolate) deformation and rapid initial rotation can make GW emission dominate angular momentum and rotational energy losses. For a given spindown torque, $\dot{\omega} = -\mathrm{K}_\alpha\omega^\alpha$, the corresponding spindown timescale is $\tau_{\mathrm{sd}} \equiv \omega/(2\dot{\omega})$. For convenience, in the following we express the relative strength of the two torques at birth in terms of the ratio:

$$\frac{\tau_{\mathrm{d},i}}{\tau_{\mathrm{gw},i}} = \frac{\mathrm{K}_{\mathrm{gw}}\omega_i^2}{\mathrm{K}_{\mathrm{d}}} = \frac{\omega_i^2}{A} \equiv x \qquad (3)$$

where $A \equiv \mathrm{K}_{\mathrm{d}}/\mathrm{K}_{\mathrm{gw}}$; GW losses are dominant for $x > 1$.

The complete spin-down equation we adopt is thus:

$$\dot{\omega} = -\frac{2}{3}\frac{\mu_d^2}{\mathrm{Ic}^3}\ \omega^3 - \frac{\dot{\mathrm{E}}_{\mathrm{gw}}}{\mathrm{I}\omega}\ \omega^5 = -\mathrm{K}_{\mathrm{d}}\ \omega^3 - \mathrm{K}_{\mathrm{gw}}\ \omega^5 \qquad (4)$$

where $\dot{\mathrm{E}}_{\mathrm{gw}}$ is given by (1), or by (2) when $\chi \approx \pi/2$.

2.1 Damping of freebody precession and orthogonalization

We consider here in some detail the very first stages when the prolate NS is formed, its symmetry axis being just slightly tilted to the spin axis. We focus in particular on those processes that might affect the orientation of the symmetry axis and thus promote (or prevent) prompt and strong GW emission.

As stated above, freebody precession of the prolate spheroid is eventually damped by internal viscous torques, which redistribute angular momentum (with no loss) inside the NS so as to minimize the spin energy. Following the analysis of Cutler (2002), Stella et al. (2005) assumed that internal (viscous) dissipation of free precession occurrs on a (very short) timescale $\tau_{\mathrm{ort}} \simeq 10^4\ \mathrm{P}_{\mathrm{prec}}$ (Alpar & Sauls 1988), where $\mathrm{P}_{\mathrm{prec}}$ (< few seconds) is the free precession period.

[1] A dipole field induces an oblate deformation with the magnetic (symmetry) axis corresponding to the largest axis of inertia. In the presence of dissipation, the figure will thus be driven towards aligned rotation and no GW emission will result.

This estimate results from the crust-core coupling caused by the interaction between superfluid neutron vortices and relativistic electrons in the NS core, where only electrons follow the instantaneous rotation of the crust. The application of this prescription to a newborn NS is subject to important caveats: neutron pairing in a $^3P_2$ state in the core occurs at a temperature $\mathrm{T_{cond}} < 2\times10^9$ K (TD96 and references therein, Page et al. 2004) and crust formation also occurs at a temperature $\sim$ a few $\times10^9$ K. The coupling mechanism studied by Alpar & Sauls (1988) does not apply when $\mathrm{T} > \mathrm{T_{cond}}$, since there is no superfluid and, likely, not even a proper crust. The NS is more like a self-gravitating, rapidly rotating, fully degenerate fluid mass. A proper account of its early cooling is thus of crucial importance in this context.

If direct Urca processes occurr in the densest parts of the core, then cooling is extremely fast due to the very large neutrino luminosity. The NS temperature drops to 10^9 K in a matter of minutes, as opposed to ~ 1 yr in the case of modified Urca cooling (cfr. Page, Geppert & Weber 2006 and references therein). Therefore, if newly born magnetars cool through direct Urca processes, crust formation and transition to superfluidity in the core occur very quickly. The crust-core coupling mechanism described by Alpar & Sauls (1988) could thus operate soon after NS birth and lead to the very short orthogonalization time estimated above.

In the opposite limit, when NS cooling is driven by only the modified Urca reactions, the evolution is more complex. The temperature in this case evolves as (Owen et al. 1998 and references therein, Page, Geppert & Weber 2006)

$$\frac{T(t)}{10^9\ K} = \left[\frac{t}{\tau_c} + \left(\frac{10^9\ K}{T_i}\right)^6\right]^{-1/6} \quad (5)$$

where $\tau_c \simeq 1$ yr and $T_i \approx 10^{10}$ K is the initial temperature of the NS at the end of the $\alpha-\Omega$ dynamo phase (TD96). As we are interested in the cooling at $\mathrm{T} > \mathrm{T_{cond}}$, no further neutrino-emitting reactions are considered, such as those occurring at $\mathrm{T}\approx \mathrm{T_{cond}}$ in the so-called "minimal cooling scenario" (Page et al. 2004 and references therein). According to eq. (5), the NS temperature will reach a value 2×10^9 K in about 5 days after formation. During this time, the crust-core coupling mechanism introduced by Alpar & Sauls (1988) cannot operate. In the absence of other viscous processes, the prolate spheroid will thus not be orthogonalized and GW emission will remain highly suppressed during those early days. Therefore magnetodipole radiation by a 10^{14} G external field will carry away most of the initial spin energy, thus spoiling the possibility of significant GW emission also at later times.

However, the prolate NS is subject to at least two further (and competing) mechanisms that can in principle alter the orientation of its symmetry axis. First, GWs will be emitted even for a small initial tilt angle χ_i, though at a small rate. The corresponding radiation reaction torque will cause the spin and magnetic axes to align, regardless of whether the spheroid is oblate or prolate (Cutler & Jones 2001). This process always acts so as to quench the GW emission efficiency.
On the other hand, freebody precession induces internal motions in the newly formed, fluid NS, that are required by the condition of hydrostatic equilibrium (Mestel & Takhar 1972; Jones 1976). Dissipation of these internal motions through bulk viscosity is potentially able to orthgonalize the symmetry axis of the spheroid (the magnetic field axis) relative to the angular momentum vector, thus increasing the efficiency of GW emission.
The relative strength of these two mechanisms will thus determine the early evolution of the angle χ and the possibility of newly formed magnetars to become efficient GW emitters. Below we study these two processes in more detail, showing that orthogonalization through bulk viscous damping is expected to always prevail on radiation reaction, in the parameter range of interest to our work.

2.1.1 ***Equation of state and related quantities***

For our aims, the equation of state (EOS throughout) of NS matter enters through its role in determining the global structural properties of the NS, such as the mass-radius relation and the moment of inertia. We dot not consider the detailed microphysics that determine the EOS; rather we adopt a phenomenological approach, parametrizing all results in terms of the NS mass and radius.
As shown by Lattimer & Prakash (2001) most NS EOS's are well approximated by a polytrope of index $n = 1$, with $P = k\rho^2$, as far as their global properties are concerned. Here k is determined by the stellar radius (see Appendix B). We also adopt the approximate formula for the NS moment of inertia given by Lattimer & Prakash (2001): $\mathrm{I}\approx 0.35MR^2 \simeq 1.4\times10^{45}(\mathrm{M}/1.4\ \mathrm{M_\odot})(\mathrm{R}/12\ \mathrm{km})^2$ g cm^2. Finally we note that, as discussed in Lattimer & Prakash (2007), internal magnetic fields weaker than $\simeq 10^{18}$ G are not expected to sizeably affect the microphysics that determine the EOS.

For the sake of completeness, we also report here the resulting relation between the measured P and $\dot{P}$ of a NS and the corresponding magnetic field strength as derived by the magnetodipole spindown formula (see eq. 4).

$$\begin{aligned}\mathrm{B_d} &\simeq 4.4\times10^{19}(\mathrm{P\dot{P}})^{1/2}\left(\frac{\mathrm{M}}{1.4\mathrm{M_\odot}}\right)^{1/2}\left(\frac{\mathrm{R}}{12\mathrm{km}}\right)^{-2}\ \mathrm{G}\\ \mu_\mathrm{d} &\simeq 3.8\times10^{37}(\mathrm{P\dot{P}})^{1/2}\left(\frac{\mathrm{M}}{1.4\mathrm{M_\odot}}\right)^{1/2}\left(\frac{\mathrm{R}}{12\mathrm{km}}\right)\mathrm{Gcm^3}\end{aligned} \quad (6)$$

2.1.2 ***The Magnetically-Induced Distortion of a Neutron Star***

One of the key parameters of interest is the deviation from spherical symmetry (ϵ_B) of the NS, that is caused by the anisotropic pressure of the internal magnetic field. This determines the frequency of freebody precession and the GW luminosity of the rapidly spinning NS. In general, ϵ_B will be determined by the volume-integrated ratio of the magnetic to gravitational binding energy densities, times some numerical coefficient accounting for field geometry and NS structure. Setting the latter factor to unity, and assuming an approximately constant density in the NS core

$$\frac{I_3 - I_1}{I_1} = \frac{\Delta I_B}{I_1} \equiv \epsilon_B = \frac{15}{4}\frac{E_\mathrm{B}}{E_\mathrm{G}} = \frac{15}{4}\mathrm{E_G^{-1}}\int\frac{B^2}{8\pi}\,dV \quad (7)$$

as determined from general arguments based on the virial theorem (Cutler 2002 and references therein). In the above definition, the integral is extended to the whole NS volume

where the magnetic field is present. We are assuming the internal field to be mostly toroidal, the poloidal component being sufficiently small to be energetically negligible, as envisaged in the millisecond magnetar formation scenario. $\mathrm{E_G}$ in eq. (7) is the gravitational binding energy of the NS that, for a polytrope of index $n = 1$, is $\mathrm{E_G} = (3/4)GM^2/R$. The value of ϵ_B can thus be approximated as

$$\epsilon_B \approx -1.15 \times 10^{-3} \left(\frac{\mathrm{E_B}}{10^{50}\ \mathrm{erg}}\right) \left(\frac{\mathrm{R}}{12\ \mathrm{km}}\right) \left(\frac{\mathrm{M}}{1.4\mathrm{M}_\odot}\right)^{-2} \quad (8)$$

that is negative for a prolate shape. The volume-averaged strength of the internal (toroidal) magnetic field is:

$$\left\langle \frac{\mathrm{B_t}}{2 \times 10^{16}\ \mathrm{G}} \right\rangle \simeq 0.93 \left(\frac{\mathrm{E_B}}{10^{50}\ \mathrm{erg}}\right)^{1/2} \left(\frac{\mathrm{R}}{12\ \mathrm{km}}\right)^{-3/2} \quad (9)$$

Uncertainties in the exact value of ϵ_B as a function of the (unknown) internal field distribution can be parametrized by adding a further multiplicative factor[2] (η) in the right-hand side of eq. (7) where, in general, $\eta > 1$ is expected. We neglect this factor for clarity, but stress that the quantity $\mathrm{E_B}$ used throughout can more generally be substituted with $\eta \mathrm{E_B}$. We explicitly assume $\eta = 1$ from here on.

2.1.3 *Gravitational radiation reaction*

The effect of gravitational radiation reaction on damping of freebody precession was investigated by Cutler & Jones (2001), who showed that GW emission always drives the tilt angle χ to zero, independent of whether the NS is oblate or prolate. In the limit of small χ, these authors express the freebody precession damping timescale ($\tau_{\rm rr}$) as:

$$\frac{\sin\chi}{\mathrm{d}(\sin\chi)/\mathrm{dt}} \equiv \tau_{\rm rr}^{\chi} = \frac{5c^5}{2G\Omega^4} \frac{I_1}{(I_1\epsilon_B)^2} \approx$$
$$\approx 3.7 \left(\frac{\mathrm{E_B}}{10^{50}\mathrm{erg}}\right)^{-2} \left(\frac{\mathrm{P}}{\mathrm{ms}}\right)^{4} \left(\frac{\mathrm{R}}{12\mathrm{km}}\right)^{-4} \quad \mathrm{d} \quad . \quad (10)$$

The importance of this effect on the early evolution of a newly formed magnetar can be determined by comparing this timescale to the bulk viscosity dissipation timescale and to the magnetodipole spindown timescale.

[2] The exact value of ϵ_B is uncertain as it depends on the magnetic field configuration and EOS. Using a general relativistic treatment of the NS structure, Bonazzola & Gourgoulhon (1996) studied the way in which the numerical factor in eq. (7) changes for different configurations of the internal magnetic field. These authors showed that this factor can be higher than 15/4, or even much higher, for specific magnetic field geometries (for example the case of an internal field that is mainly concentrated in an outer shell of the NS core, or the case of an intermittent field distribution rather than a uniform one). Haskell et al. (2008) studied the same problem allowing for different EOS's and combinations of the toroidal and poloidal components of the internal field. Their results confirm that the magnetically-induced ellipticity can be in general somewhat larger, or significantly larger in particular cases, than the estimate given by eq. (7) and (8).
Overall then, for a given magnetic energy, larger ellipticities than given by eq. (7) are a possibility worth of further investigations.

2.1.4 *Bulk viscosity in newly born NSs*

As shown by Mestel & Takhar (1972), a field of internal motions is excited in order to maintain hydrostatic equilibrium everywhere within a fluid star undergoing freebody precession. These motions are periodic, with the same frequency as freebody precession and amplitude proportional to the (non-spherical) centrifugal deformation of the star ($\rho_\Omega \propto \Omega^2$) and tilt angle χ of the magnetic axis. In this section we discuss the damping of such motions by bulk viscosity and the associated growth of the tilt angle χ, within a non-superfluid NS made only of neutrons, protons and electrons (*npe* matter).

The assumption of pure *npe* matter corresponds to the least favourable case for damping through bulk viscosity and likely not the most realistic. At the highest densities of NS cores muons and possibly hyperons (Λ, Σ^-) are expected to appear, significantly increasing the bulk viscosity coefficient (e.g. Jones 1976; Lindblom & Owen 2002 and references therein). In this respect, our calculations are conservative. Detailed models should lead to significantly shorter damping times for the excited modes.
Fluid bulk viscosity is a consequence of the finite time it takes for the fluid to react to changes in one of its thermodynamic parameters, adjusting the others to their new equilibrium values. In hot NS matter, displacement of a fluid parcel from the equilibrium position causes departure from chemical equilibrium between particle species: bulk viscosity is thus determined by the activation of β-reactions trying to restore chemical equilibrium. A general expression for the bulk viscosity coefficient in NS matter (ζ) has been derived by Lindblom & Owen (2002)

$$\mathrm{Re}(\zeta) = \frac{n\tau \left(\partial p/\partial x\right)_n d\tilde{x}/dn}{1 + (\omega\tau)^2} \simeq \frac{n \left(\partial p/\partial x\right)_n d\tilde{x}/dn}{\omega^2\tau} \quad , \quad (11)$$

where n is the particle density, p is the pressure (whose derivative is calculated at constant proton fraction, $x = n_p/n_n \simeq n_p/n$) and $\tilde{x}$ is the equilibrium value of x. The quantities in the denominator are the mode frequency ($\omega_{\rm pre} \sim \epsilon_B \Omega_{\rm spin}$) and β-reaction timescale (τ_β). Defining the characteristic damping time of the excited motions as $\tau_{\rm d} \equiv 2\mathrm{E_{pre}}/|\dot{\mathrm{E}}_{\rm pre}|$ one can express it as (cf. Owen et al. 1998)

$$\tau_{\rm d} = \left(\frac{\int \zeta |\vec{\nabla}\cdot\vec{\delta v}|^2\ \mathrm{dV}}{2\ \mathrm{E_{pre}}}\right)^{-1} = \frac{1}{\omega_{\rm pre}^2} \left(\frac{\int \zeta (\delta\rho/\rho)^2\ \mathrm{dV}}{2\ \mathrm{E_{pre}}}\right)^{-1} , \quad (12)$$

where $\vec{\delta v}$ is the velocity perturbation associated to the mode. In the last step we have used the relation $\vec{\nabla}\cdot\vec{\delta v} = i\omega(\Delta n/n)$ (Lindblom & Owen 2002) and substituted the Eulerian perturbation, $\delta\rho$, to the Lagrangian one, $\Delta\rho$. A word of caution is needed here. The analysis by Mestel & Takhar (1972) gives $\nabla\cdot\vec{\xi} = 0$, *i.e* $\Delta\rho = 0$ and $\delta\rho = -\vec{\xi}\cdot\nabla\rho$, a condition that would imply the absence of bulk viscosity. However, this result is a direct consequence of having considered strictly adiabatic fluid motions[3] within a radative (sub-adiabatic) layer, in a first-order perturbative analysis. As opposed to this, a polytropic NS would have an almost adiabatic gradient, in which case the calculations by Mestel & Takhar would leave $\nabla\cdot\vec{\xi}$ totally unconstrained, revealing the need for a higher-order pertubation analysis. Indeed these authors

[3] In fact, bulk viscosity is a result of deviations from strict adiabaticity of perturbations.

discuss the (non)applicability of their conclusion to a convective (almost adiabatic) zone, at the end of their section 3. They discuss a number of approximations in their analysis that may well break in the case of a very rapid rotator (such as a millisecond magnetar) thus introducing non-negligible higher-order terms in the perturbations. In these cases, the internal dynamics of the oblique rotator becomes much more complicated and a detailed analysis is beyond our scope here.

In general, however, motions of the same order of magnitude as the one discussed by Mestel & Takhar (1972) are always expected to occur, whose rate of expansion $(\nabla \cdot \vec{\xi})$ must be calculated explicitly. Here, in analogy to Reisenegger & Goldreich (1992) and to several treatments of bulk viscosity for r-modes (Lindblom, Owen & Morsink 1998; Owen et al. 1998), we assume that $\Delta\rho$ would be of the same order of magnitude of $\delta\rho$, leaving more detailed analyses to future work. To stress the importance of this aspect we note that Lindblom, Mendell & Owen (1999) carried out a second-order analysis for r-mode damping through bulk viscosity and derived an order of magnitude longer dissipation timescale than those based on the assumption $\Delta\rho \sim \delta\rho$.

We finally note that $\delta v \sim \epsilon_B \omega R \sim 10^7$ cm s^{-1}, while the Alfvèn velocity is $v_A = B/\sqrt{4\pi\rho} \sim (10^8 \div 10^9)$ cm s^{-1} for the parameters of interest. Alfvèn waves are thus very efficiently in maintining rigid rotation of the fluid star, despite the perturbation in principle introduced by $\vec{\xi}$.

The calculation of the perturbation amplitude $(\delta\rho/\rho)$ is detailed and discussed in Appendix B. We report here our result for the damping timescale of freebody precession according to eq. (12)

$$\tau_{\rm d} \simeq 13.5 \frac{\cot an^2\chi}{1+3\cos^2\chi} \left(\frac{\rm E_B}{10^{50}{\rm erg}}\right) \left(\frac{\rm P}{\rm ms}\right)^2 \left(\frac{\rm M}{1.4\ {\rm M}_\odot}\right)^{-1} \left(\frac{\rm T}{10^{10}{\rm K}}\right)^{-6} {\rm s}\ , \quad (13)$$

a fairly short time even for small initial values of the tilt angle (χ_i).

Given $\tau_{\rm d}$, we can eventually calculate the growth time of the tilt angle, $\tau_{\rm d}^{\chi}$. As shown in Appendix A damping of freebody precession reduces the NS spin energy, at a constant angular momentum, by changing the tilt angle χ. From eq. A9 we get:

$$\tau_{\rm d} = \frac{\cos\chi}{\dot{\chi}\ \sin\chi} = \frac{\cos^2\chi}{\sin^2\chi} \frac{\sin\chi}{{\rm d}(\sin\chi)/{\rm dt}} = \cot an^2\chi\ \tau_{\rm d}^{\chi}\ . \quad (14)$$

Here, $\tau_{\rm d}^{\chi}$ is the timescale to be compared to $\tau_{\rm rr}^{\chi}$ (eq. 10) in order to determine the relative importance of bulk viscosity and radiation reaction in the evolution of χ. In the limit of small tilt angle, for which $\cos\chi \simeq 1$, we have

$$\frac{\tau_{\rm d}^{\chi}}{\tau_{\rm rr}^{\chi}} \approx 10^{-5} \left(\frac{\rm E_B}{10^{50}\ {\rm erg}}\right)^3 \left(\frac{\rm P}{\rm ms}\right)^{-2} \left(\frac{\rm T}{10^{10}{\rm K}}\right)^{-6} \left(\frac{\rm R}{12{\rm Km}}\right)^4 \quad (15)$$

From this we derive the condition for bulk viscosity to largely prevail on gravitational radiation reaction, so that orthogonalization is essentially unaffected by radiation-reaction. For definiteness we require $\tau_{\rm d}^{\chi} < 0.1\tau_{\rm rr}^{\chi}$, a condition that translates to

$${\rm E_B} \leqslant 2.3 \times 10^{51} \left(\frac{\rm T}{10^{10}{\rm K}}\right)^2 \left(\frac{\rm P}{\rm ms}\right)^{2/3} \left(\frac{12{\rm km}}{\rm R}\right)^{4/3} {\rm erg} \quad (16)$$

or[4] ${\rm B} < 9 \times 10^{16}\ ({\rm T}/10^{10}{\rm K})\ ({\rm P_{ms}})^{1/3}$ G.

Soon after formation, the temperature T decreases on a very short timescale, not much different from $\tau_{\rm d}^{\chi}$ itself, even for the slow cooling given by eq. (5). The angle χ and T thus evolve on comparable timescales and just considering the damping timescale at a given temperature is not appropriate. Rather, the coupled evolution of χ and T must be solved in order to derive a reliable estimate of the time it takes for χ to grow to large values.

Inserting the cooling history (5) in (13) or (14), the resulting equation for χ can be solved with initial conditions $\chi = \chi_i$ and ${\rm T}_i = 10^{10}$ K. Since $\tau_{\rm d}(t) = {\rm N}\ T_{10}^{-6}(t)\ \cos^2\chi/[\sin^2\chi(1+3\cos^2\chi)]$, the expression ${\rm T}_{10}^{-6}({\rm t}) = [({\rm t}/30)+1]$ gives:

$$\frac{\cot an\chi}{1+3\cos^2\chi}{\rm d}\chi = \frac{\rm dt}{{\rm N}\left(\frac{t}{30}+1\right)} \quad (17)$$

whose solution is:

$$\frac{\sin^2\chi}{1+3\cos^2\chi} = \frac{\sin^2\chi_i}{1+3\cos^2\chi_i}\left(\frac{t}{30}+1\right)^{240/{\rm N}} = = \frac{\sin^2\chi_i}{1+3\cos^2\chi_i}\ T_{10}^{-1440/{\rm N}} \quad (18)$$

From the above we can obtain the time (in seconds) or the temperature (in units of 10^{10} K) at which a sufficiently large value of the angle χ is reached starting from a given, small initial tilt angle χ_i.

The requirement that the damping time of free precession be much shorter than the initial spindown timescale of the NS allows two key constraints to be met jointly and our scenario to maintain full self-consistence; first, damping of free precession will be well described in terms of the approximation of constant angular momentum. Second, efficient GW emission will ensue quick enough for the NS *initial* spin energy to be still fully available.

The initial timescale for electromagnetic spindown is $\tau_{\rm em}^i \simeq 1.1\ P_{\rm ms}^2 B_{\rm d,14}^{-2}$ d, and in a time $\simeq 0.1\tau_{\rm em}^i$ less than 10% of the initial spin energy is lost to magnetic dipole radiation. Hence, we consider this as the longest time over which orthogonalization must take place for our scenario to apply. Therefore, given $\chi_i = 1$ deg, the angle χ will grow to a sufficiently large value - say, $\chi = 60$ deg[5] - in a time shorter than $0.1\ \tau_{\rm em}^i$, if[6]

$$\frac{\rm E_B}{10^{50}\ {\rm erg}} < 2.1 \frac{\rm M_{1.4}}{\rm P_{ms}^2}\left[\ln\left(320\ {\rm M_{1.4}R_{12}^{-4}}\frac{\rm P_{ms}^2}{\rm B_{d,14}^2}+1\right)\right] \simeq 4.2 \frac{\rm M_{1.4}}{\rm P_{ms}^2}\left(3+\ln\frac{\rm P_{ms}}{\rm B_{d,14}}+\ln\frac{\rm M_{1.4}}{\rm R_{12}^4}\right) \quad (19)$$

Note that the numerical coefficient in the last step is ~ 5 if $\chi_i = 2$ deg, and ~ 2.8 if $\chi_i = 0.1$ deg.

[4] For small χ the temperature is always very near to 10^{10} K. Therefore, this constraint is easily met if B is not very close to 10^{17} G.

[5] For $\chi \simeq 60$ deg GW emission is very efficient and can be approximated by eq. (2)

[6] Note that for any ${\rm B_d} \geqslant 6\times10^{13}$ G and ${\rm P}_{i,{\rm ms}} \leqslant 3$ ms, $0.1\tau_{i,{\rm em}} \leqslant 3$ days. The core temperature will accordingly be $> 2 \times 10^9$ K, so that our condition covers essentially the range of temperature before the core becomes superfluid.

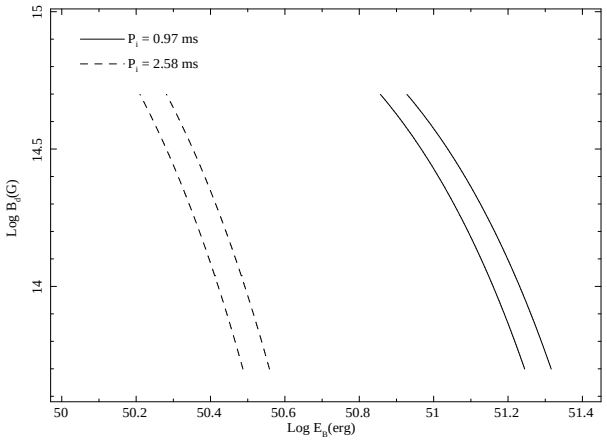

Figure 1. The region of parameter space, in the external dipole field strength (B_d) vs. internal magnetic energy (E_B), where the timescale for the angle χ to grow to a large value (60 deg) is less than one tenth of the initial spindown timescale through magnetodipole radiation. The favourable region lies on the left of the corresponding limiting curve. For each value of the initial spin period, two curves are plotted for two different values of the initial tilt angle, $\chi_i = 1$ (left) and 2 deg (right). Note that further decreasing χ_i from 1 deg to 0.1 deg shifts the curves to the left by a slightly larger amount than the decrease of χ_i from 2 deg to 1 deg (cfr. eq. 19). This would still leave ample room in parameter space for the fastest spinning magnetars, while it would drastically reduce the available parameter space for magnetars with $P_i \geqslant 2.5$ ms.

Eq. (19) is represented in Fig. 1 by two curves corresponding to initial spin periods of 0.97 and 2.58 ms, that approximately bracket the relevant range of spin periods for newly formed magnetars. Each curve is plotted for two different values of the initial tilt angle, $\chi_i = 1$ and 2 deg (see caption for further details).

The constraint shown in Fig. 1 will be used, together with independent constraints derived in later sections, to identify the region in parameter space where GW emission efficiency from newly formed magnetars is optimized. We stress again here that all our calculations were carried out by assuming pure *npe* matter, a conservative assumption that minimises the efficiency of bulk viscosity. Finally, in Appendix B we calculate the centrifugal distortion of the density profile in the slow-rotation limit, which is also likely to underestimate the deformation of a millisecond magnetar. This translates into an underestimate of $\delta\rho$ in eq. (12) and, thus, of the efficiency of bulk viscosity.

We conclude that, despite having chosen a "worst case approximation", damping of freebody precession through bulk viscosity in a newly formed, rapidly spinning and strongly magnetized NS can be very efficient in the parameter range considered here. Therefore, strong GW emission from an almost orthogonal, rapidly rotating NS is likely to ensue quickly as a consequence of a strong toroidal magnetic field *and* of the efficient dissipation of its freebody precession energy. The implications of this are explored further in the next section.

3 AMPLITUDE AND DETECTABILITY OF THE EMITTED SIGNAL

Stella et al. (2005) calculated the expected signal-to-noise ratio (S/N) that a putative GW signal from a newly born magnetar would have, for an optimal (matched-filter) detection, adopting the broadband design sensitivity of Advanced Ligo. At frequencies between 0.5 and 2 kHz this is well approximated by

$$S_h(f) \approx S_0 \; f^2 \quad , \tag{20}$$

where $S_h(f)$ represents the one-sided spectral noise distribution of the detector, $f = 2\omega$ the GW signal frequency and $S_0 \simeq 2.1 \times 10^{-53}$ Hz^{-1} (Owen & Lindblom 2002; Cutler 2002 and references therein). Note that the designed sensitivity for Advanced Virgo is very similar, in this range of frequencies (Losurdo 2007), so that our calculations hold essentially for both detectors. frequency, $f = \omega/\pi$ for an orthogonal prolate rotator.

We re-address here this point to better qualify the role of the NS ellipticity in the detectability of the signal. We also correct a (small) numerical error in the calculated S/N curves in Fig. 1 of Stella et al. (2005), whose conclusions maintain their general validity. The S/N of an optimal signal search is defined as

$$\mathrm{S/N} = 2 \left[\int \frac{|\tilde{h}(f)|^2}{S_h(f)} \right]^{1/2} \quad . \tag{21}$$

Here $\tilde{h}(f)$ is the Fourier transform of the instantaneous signal strain $h[f(t)]$ that, in the stationary phase approximation, is expressed as (cfr. Owen & Lindblom 2002 and references therein)

$$|\tilde{h}(f)|^2 = \frac{1}{2} h^2[f(t)] \left| \frac{\mathrm{d}f}{\mathrm{dt}} \right|^{-1} \quad , \tag{22}$$

where the time derivative of f is obtained from eq.(4), since $\dot{f} = \dot{\omega}/\pi$. We adopt the expression for the strain amplitude - averaged over source orientation - given by[7] Ushomirsky, Cutler & Bildsten (2000):

$$h_a(f) = \frac{16}{5} \left(\frac{\pi^3}{3} \right)^{1/2} \frac{\mathrm{GI}\epsilon_B}{\mathrm{Dc}^4} \; f^2 \quad , \tag{23}$$

where D is the source distance. Further averaging over the detector antenna pattern, eq. (21) gives the optimal S/N ratio:

$$\mathrm{S/N} = \sqrt{\frac{2}{5}} \left[\int \frac{h^2(t)}{S_h(f) \; \mathrm{d}f/\mathrm{dt}} \right]^{1/2} = $$
$$= \frac{4}{5} \sqrt{\frac{\pi \mathrm{GI}}{6\mathrm{c}^3}} \frac{\pi}{\mathrm{DS}_0^{1/2}} \left(\frac{\mathrm{K_{gw}}}{\mathrm{K_d}} \right)^{1/2} \left[2 \; \ln \frac{f_i}{f_f} - \ln \frac{a + f_i^2}{a + f_f^2} \right]^{1/2} \tag{24}$$

where we have set $a = \mathrm{K_d}/(\pi^2 \mathrm{K_{gw}}) = A/\pi^2$. Substituing the numerical values:

$$\mathrm{S/N} \approx \quad 6 \left(\frac{\mathrm{E_B}}{10^{50}\mathrm{erg}} \right) \left(\frac{\mathrm{B_d}}{10^{14}\mathrm{G}} \right)^{-1} \left(\frac{\mathrm{R}}{12\mathrm{km}} \right) \left(\frac{\mathrm{M}}{1.4\mathrm{M}_\odot} \right)^{-1/2}$$
$$\left(\frac{\mathrm{D}}{20\mathrm{Mpc}} \right)^{-1} \left[2 \ln \frac{f_i}{f_f} + \ln \frac{a+f_i^2}{a+f_f^2} \right]^{1/2} \tag{25}$$

[7] Comparing with the "optimally-oriented" strain amplitude h_0 given by Abbot et al. (2007), we obtain the relation $h_a = 4/(5\sqrt{3\pi}) h_0$.

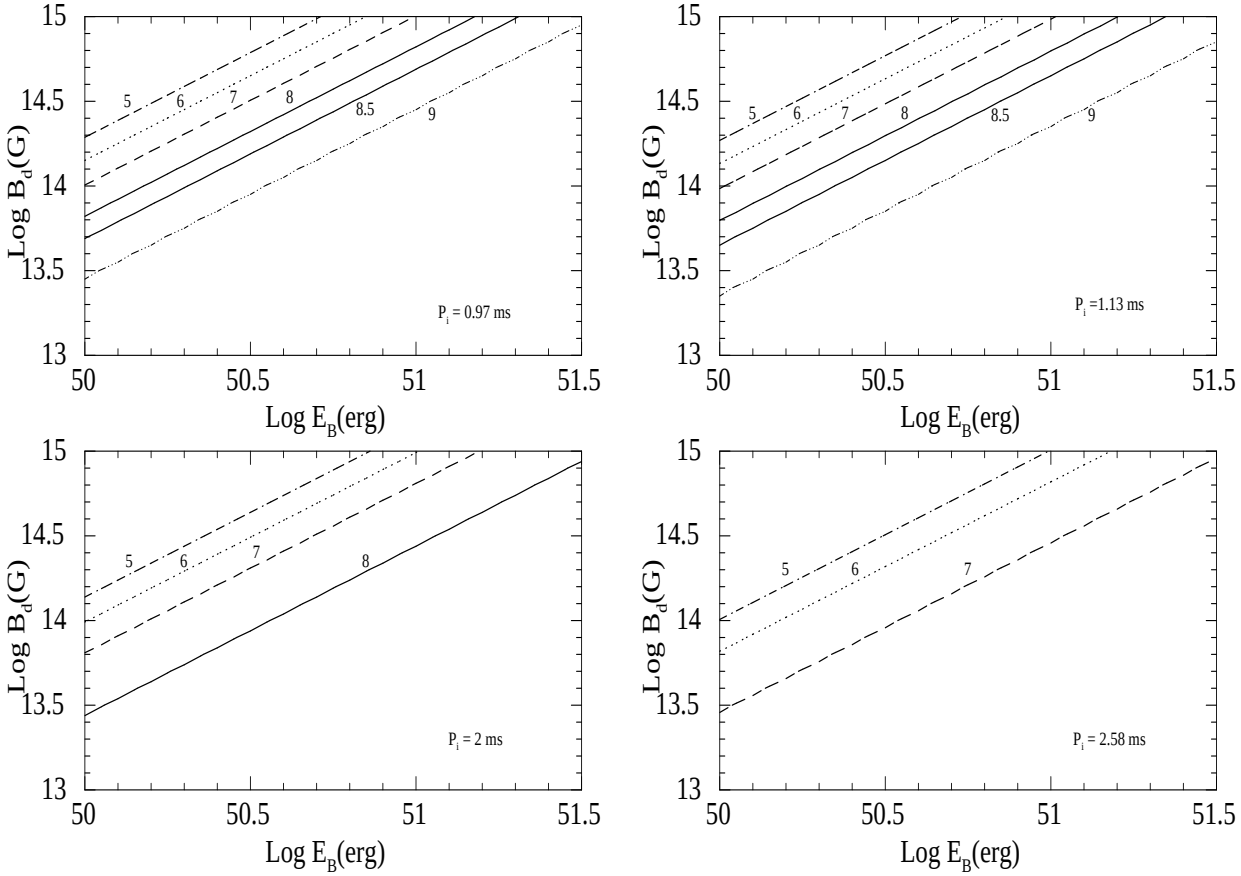

Figure 2. The optimal (matched-filtered) signal-to-noise for searches of the GW signal from newly formed magnetars in the Virgo Cluster with Advanced Ligo /VIrgo, calculated through eq. (25). Four different values of the initial spin (indicated in the figures) are considered and results are shown as contour levels (at the values of S/N indicated on each line) in the B_d vs. E_B plane.

In Fig. 2 we show the curves of constant S/N in the B_d vs. E_B for selected values of the initial spin, as derived from eq. (25). More details are given in the caption. According to eq. (24) the *maximum* S/N is obtained in the limit $a \to 0$, which depends *only* on the initial spin energy of the NS *and not* on its oblateness. Clearly, this value $[S/N]_{MAX}$ is attained as the magnetodipole spin-down torque disappears, so that all of the initial spin energy of the NS is lost to GWs. This can also be seen directly by substituting the expression for the pure GW-driven spindown in eq. (24), which gives

$$[S/N]_{MAX} \simeq 4.5 \left(\frac{D}{20Mpc}\right)^{-1} \left(\frac{R}{12Km}\right) \left(\frac{M}{1.4M_\odot}\right)^{1/2} \left[\left(\frac{f_f}{kHz}\right)^{-2} - \left(\frac{f_i}{kHz}\right)^{-2}\right]^{1/2} \quad (26)$$

3.1 Quantifying the gravitational and electromagnetic energy output

Thus far we have discussed the conditions under which the hypothesis that newly born magnetars be detectable sources of GWs with next generation detectors can be true. X-ray observations of Supernova Remnants (SNRs) around magnetar candidates in the Galaxy give us clues on the actual viability of this hypothesis (cf. § 1). In this section, we show that our scenario is indeed fairly consistent with such observations. We find that, if magnetars at birth were *detectable* sources of GWs from Virgo-cluster distance, then SNRs around them would likely show no significant excess of energy injection with respect to "ordinary" SNRs[8]

We begin calculating the total integrated energy emitted via GWs by a newly born magnetar as:

$$\Delta E_{gw} = -\int_{t_i}^{\infty} \dot{E}_{gw}\, dt = \int_0^{\omega_i} \frac{\dot{E}_{gw}}{\dot{\omega}}\, d\omega \quad (27)$$

For the spindown model in eq. (4), the above integral gives

$$\Delta E_{gw} = I \int_0^{\omega_i} \frac{\omega^3}{\omega^2+A}\, d\omega = I \left[\frac{\omega^2}{2} - \frac{A}{2}\ln(\omega^2+A)\right]_0^{\omega_i} = E_{spin,i}\left[1 - \frac{A}{\omega_i^2}\ln\left(1+\frac{\omega_i^2}{A}\right)\right] \quad (28)$$

Eq. (28) expresses ΔE_{gw} as a fraction (δ) of the initial spin energy of the NS. The remaining energy $\Delta E_{em} = E_{spin,i}(1-\delta)$ is the maximum that can be transferred to the SN ejecta. Next, we define the quantity $\Delta E_{tr} = \beta \Delta E_{em}$ as the amount of that energy that is effectively transferred to the ejecta. In the absence of additional competing torques and/or a physical prescription for the transfer mechanism, we will assume it to be perfectly efficient ($\beta = 1$), although

[8] Assuming GWs do not appreciably transfer energy to the Supernova ejecta

leaving the explicit dependence on β in the calculations that follow.
Recalling the definition of x as the ratio of gravitational to magnetic dipole torque *at birth* (eq. 3) and using eq. (28) we then get

$$\frac{\ln(1+x)}{x} = \frac{\Delta \mathrm{E_{em}}}{\mathrm{E_{spin},}i} = \frac{1}{\beta}\frac{\Delta \mathrm{E_{tr}}}{\mathrm{E_{spin},}i} \leqslant \frac{1}{\beta}\frac{E_{SNR}^{\mathrm{inj}}}{\mathrm{E_{spin},}i} \qquad (29)$$

where E_{SNR}^{inj} is the amount of energy transferred to the ejecta as determined from observations (Vink & Kuiper 2006). Observations provide an upper bound to this quantity, from which the inequality in the last step in eq. (29) obtains. We derive constraints on magnetar parameters at birth by using the upper bound determined by Vink & Kuiper (2006) discussed in this paper and our GW emission scenario.

First fix a value for x: eq. (29) gives the maximum value of the initial spin energy or, equivalently, $(\omega_i^2)_{\max}$ compatible with the upper limit on $\mathrm{E_{SNR}^{inj}}$. Accordingly, the maximum value of $A = (\omega_i^2)_{\max}/x$ is constrained (cfr. eq. 3):

$$A_{\max} = \frac{(\omega_i^2)_{\max}}{x} = \frac{2\mathrm{E_{SNR}^{inj}}}{\beta \mathrm{I}\ \ln(1+x)} \qquad (30)$$

Inserting eq. (30) in the definition of A= $\mathrm{K_d}$/ $\mathrm{K_{gw}}$ (cfr. § 2) we get the following condition, for the electromagnetic output of a newly born, millisecond spinning magnetar to be always $\leqslant 10^{51}$ erg:

$$\mathrm{E_B} \geqslant \sqrt{\frac{\mathrm{G}}{117.6\ A_{\max}}}\mathrm{McB_d} = \sqrt{\frac{\beta \mathrm{G}\ \ln(1+x)}{672\ \mathrm{E_{SNR}^{inj}}}}\mathrm{cM}^{3/2}\mathrm{RB_d} \approx$$
$$\approx 1.6\times 10^{50}\sqrt{\beta \ln(1+x)}\left(\frac{\mathrm{B_d}}{10^{14}\mathrm{G}}\right)\left(\frac{\mathrm{M}}{1.4\ \mathrm{M_\odot}}\right)^{3/2}$$
$$\left(\frac{\mathrm{R}}{12\mathrm{km}}\right)\left(\frac{\mathrm{E}_{SNR}^{\mathrm{inj}}}{10^{51}\mathrm{erg}}\right)^{-1/2} \qquad (31)$$

Therefore, given x one obtains ω_i and, eventually, the appropriate curve in the $\mathrm{B_d}$ vs. $\mathrm{E_B}$ plane. Results are shown in Fig. 3, where curves in the B_d vs.$\mathrm{E_B}$ plane have been drawn for four different values of $x = 10, 22, 100$ and 150, corresponding to the initial spins indicated in each plot. Curves of given signal-to-noise ratio from Fig. (2) are also plotted together with curves defining the region where the orthogonalization timescale is sufficiently fast (see Fig. 1).

We conclude that there exists a wide region of the parameter space where all constraints for efficient GW emission from newly born, millisecond spinning magnetars are met jointly.

4 ELECTROMAGNETIC SPIN-DOWN AT BIRTH

The ideal magnetodipole spindown formula (cfr. eq. 4) implies that a sizeable fraction of the initial spin energy of a millisecond spinning magnetar would be lost to electromagnetic emission, for $\mathrm{B_d} \geqslant 3\times 10^{14}$ G.

SGRs, and two out of seven AXPs, have spin periods and period derivatives leading to estimated dipole fields of a few times 10^{14} G, up to $\sim 10^{15}$ (cfr. Woods & Thompson 2006 and references therein), some of which are apparently out of the optimal range for GW emission at birth, if they maintained their dipole field since then. Although relation (4) is certainly true to a good degree of approximation, the ideal magnetodipole formula does not appear to hold exactly in the few isolated NSs for which sufficiently accurate timing measurements exist.

Observations show that the spin-down of pulsars, assumed to be wholly due to an electromagnetic torque, might be a somewhat weaker function of the spin frequency than expected in the ideal case. Indeed, in the few pulsars where the second time derivative of the spin frequency ($\ddot{\nu}$) could be measured, a "braking index" $n = (\ddot{\nu}\nu/\dot{\nu}^2) < 3$ is typically derived. In particular, the Crab pulsar has a measured $n = 2.5$ (Lyne, Pritchard & Smith 1988) and PSR J1119-6127 has $n = 2.9$ (Camilo et al. 2000). Livingstone et al. (2007) have recently measured braking indices of three relatively young X-ray pulsars. Again, all results give $n < 3$ (2.14 for PSR B0540-69, 2.84 for PSR B1509-58 and 2.65 for PSR J1846-0258). The Vela pulsar has the largest known deviation from the ideal case, with $n = 1.4$ (Lyne et al. 1996), although subtraction of the frequent glitches from its spin history presents difficulties and that result should be taken with some caution.
Similar (or even greater) uncertainties are associated to the putative $n \simeq 6$ determined by Marshall et al. (2004) for PSR J0537-6910 (the "Big Glitcher"). This source is found to exhibit very frequent glitches; post-glitch "recoveries" are known to significantly affect the second time derivative of the spin frequency. For this reason, the measured values of $\ddot{\nu}$ from such a frequent glitcher are probably unsuitable to determine reliably the "true" secular spindown trend. Middleditch et al. (2006) discuss in detail several aspects concerning the timing properties of this source, arguing for a much smaller value of n.

The examples of $10^3 \div 10^4$ yrs old pulsars with braking indices lower than 3 suggest considering the same possibility for magnetar candidates, which indeed have similar ages and similarly high glitch activity (Dall'Osso et al. 2003; Israel et al. 2007; Dib et al. 2008). No measurements of n has yet been obtained for AXPs and SGRs. It would be interesting to know from the data whether these sources share this same spindown property of other isolated NSs.

Several mechanisms able to produce a braking index smaller than 3 have been proposed in the literature, since the early measurements of n in the Crab pulsar. Blandford & Romani (1988) discuss in general the effects of evolving the parameters of the magnetodipole torque. They identify a secular increase in the surface magnetic field, at least over the first $\sim 10^3 \div 10^4$ years, as a most promising explanation for $n < 3$ in young NSs. Amplification of crustal fields through a thermomagnetic battery over this early phase had been previously discussed (Blandford, Applegate & Hernquist 1983 and references therein), which could find application also in this context.
Alternatively, several suggestions have been made for a secular increase of the tilt angle between the magnetic dipole and the spin axis, based on a wide variety of physical mechanisms (Goldreich 1970; Ruderman 1991; Link, Epstein & Baym 1992; Ruderman, Zhu & Chen 1998). More recently, the possibility that the zone of closed field lines in the magnetosphere (the corotating region) does not reach the light cylinder has been widely discussed,

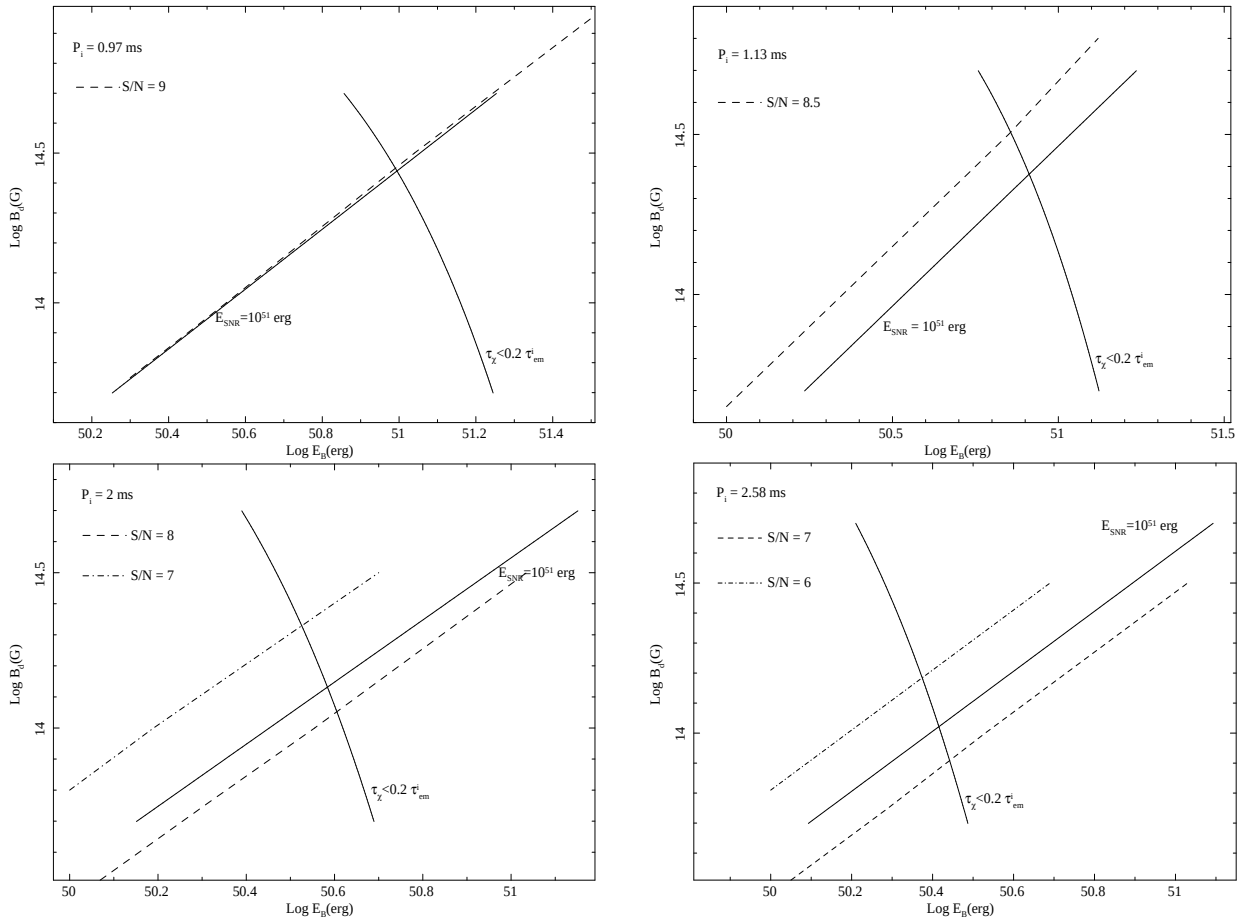

Figure 3. Curves defining the region of parameter space - in the B_d vs. E_B plane - where all constraints for efficient emission and detection of GWs are fulfilled, for four initial spin periods. The region on the left of (and below) the solid curve labelled $\tau_\chi < 0.1\tau^i_{\rm em}$ is where the tilt angle χ becomes $\geqslant 60$ deg in less than one fifth of the initial magnetodipole spindown time. The region on the right of (and below) the straight, solid curve is where the energy emitted electromagnetically by the newly formed magnetar is $\leqslant 10^{51}$ erg. It is obtained from eq. (31) with four different values of $x = 150, 100, 22, 10$ from top to bottom and right to left, corresponding to the initial spins indicated in the figures. The region on the right of the dashed (or dot-dashed) curves is where a match-filtered search with Advanced LIGO/Virgo would give a signal-to-noise ratio greater than indicated in the figures, with the source at the distance of the Virgo Cluster (20 Mpc).

both in the general context of studies of pulsar magnetospheres (Contopoulos, Kazanas & Fendt 1999; Gruzinov 2006; Contopoulos & Spitkovsky 2006; Spitkovsky 2006) and in relation to the magnetospheric structure of newly born magnetars (Bucciantini et al. 2006; Metzger et al. 2007).

Simulations by Spitkovsky (2006) have shown that the closed field line region reaches the light cylinder in a matter of one (at most) rotation period, as a model NS is set into rotation. However, it is not obvious whether the region of closed field-lines can subsequently track the expansion of the light cylinder as the NS spins down or, rather, lag behind it at an increasing distance, which would naturally lead to $n < 3$ (Contopoulos & Spitkovsky 2006 and references therein).

Without indicating any particular mechanism, we discuss the consequences that an electromagnetic braking index $n < 3$ would have, at a purely phenomenological level.
Considering a generic model for electromagnetic spindown with braking index n, one has

$$\dot{\omega}^{(n)} = -{\rm K}_{\rm d}^{(n)}\ \omega^n \quad , \tag{32}$$

where the constant ${\rm K}_{\rm d}^{(n)} = (\dot{\omega}_0/\omega_0^n)$ and the subscript "0" refers to present-day values of the parameters. According to eq. (32), given measured timing parameters $(\omega_0, \dot{\omega}_0)$ of a source the expression for its spindown at birth in the case $n \neq 3$ and case $n = 3$ are related through

$$\dot{\omega}_i^{(n)} = -{\rm K}_{\rm d}^{(n)}\omega_i^n = -{\rm K}_{\rm d}^{(3)}\omega_0^3\left(\frac{\omega_i}{\omega_0}\right)^n = \dot{\omega}_i^{(3)}\left(\frac{\omega_i}{\omega_0}\right)^{n-3} \quad , \tag{33}$$

where the subscript "i" indicates quantities at birth.
Note that the quantity in parentheses is smaller than unity for $n < 3$. It is therefore natural to ask what value of n would be required in magnetar candidates (AXPs/SGRs), given their measured ω_0 and $\dot{\omega}_0$, for their spindown *at birth* to have been dominated by GW emission rather than by the magnetic dipole radiation.

In order to answer this, we define the maximum allowed strength of the electromagnetic spindown at birth ($\dot{\omega}_{i,\rm max}$). Given the results of the previous section, this maximum value will equal that the ideal magnetodipole formula (n =3) would give for $B_d = B_d({\rm max}) = 2{\times}10^{14}$ G (a value that guarantees strong GW emission at birth, cfr. § 3.1). Therefore

we write, $\dot{\omega}_{i,\max} = \mathrm{K}^{(3)}_{\mathrm{d,max}}\ \omega_i^3$ and the last step of eq. (33) must be smaller than $\dot{\omega}_{i,\max}$, which gives:

$$\mathrm{K}^{(3)}_{\mathrm{d}} \left(\frac{\omega_i}{\omega_0}\right)^{n-3} \leqslant \mathrm{K}^{(3)}_{\mathrm{d}}(\max) \qquad (34)$$

From this, since the ratio of the torque functions corresponds to the ratio of the magnetic dipole fields:

$$\begin{aligned}(3-n)\mathrm{Log}\left(\frac{\omega_i}{\omega_0}\right) &\geqslant 2\ \mathrm{Log}\left(\frac{\mathrm{B_d}}{\mathrm{B_d\ (max)}}\right) \qquad \text{or} \\ n &\leqslant 3 - 2\ \frac{\mathrm{Log}\left[\mathrm{B_d}/\mathrm{B_d(max)}\right]}{3 + \mathrm{LogP_0} - \mathrm{LogP}_{i,\mathrm{ms}}} \qquad (35)\end{aligned}$$

Among SGRs and AXPs, SGR 1806-20 has the strongest inferred dipole field ($\simeq 1.1 \times 10^{15}$ G with R= 12 km and M= $1.4\mathrm{M}_\odot$, cfr. Woods & Thompson 2006), thus requiring the largest deviation from $n = 3$ in the hypothesis discussed here. Even assuming a (relatively) slow initial spin period for this source, $\mathrm{P}_i = 3$ ms, eq. (35) gives $n \leqslant 2.6$, a wholly plausible value compared to other isolated NSs. Note that the constraint is slightly weaker for other SGRs and/or considering a spin period at birth shorter than 3 ms. For AXPs, the limit on n ranges from 2.7 to 2.85, for an (unfavourable) initial spin of 3 ms. This speculative argument would require direct measurements of braking indices in magnetar candidates. However, our aim here was to emphasize the dependence (strong, in some cases) of the calculations of previous sections on a number of poorly constrained physical parameteres, and the importance of further studies on all of the above aspects.

5 THE DECAY OF CORE FIELDS IN THE 10^{16} G RANGE

The secular evolution (and dissipation) of the magnetic field in NS cores was studied in detail by Goldreich & Reisenegger (1992) (GR92 from here on) and their analysis was extended by TD96 to the specific case of magnetar fields in the 10^{15} G range. In magnetars, large-scale field instabilities leading to fast dissipation events were studied in detail as well (TD95; TD01; Lyutikov 2003), in order to interpret the powerful bursts and flares of SGRs.

In GR92 three separate processes for secular field evolution were identified two of which, ohmic dissipation and ambipolar diffusion, are dissipative while the third, Hall drift, conserves magnetic energy. In particular, ambipolar diffusion was found to be more sensitive to the field intensity (GR92) which in fact implies that, while this process is not very important in normal NSs, it is the main mechanism for direct field decay in magnetars (TD96).

Hall drift can affect indirectly the evolution and dissipation of magnetic fields in NS interiors, on longer timescales than those characteristic of ambipolar diffusion (TD96; Arras et al. 2004). As suggested in GR92 (and recently studied in detail by Cumming et al. 2004), excited Hall modes of field diffusion could decay (or cascade) to shorter wavelenghts, that are subject to enhanced ohmic dissipation. This has particular relevance for accelerating field decay in a magnetar's crust, as recent studies pointed out (Pons et al. 2007; Pons & Geppert 2007). Furthermore, Hall diffusion can drive - yet conserving the total energy - an initially stable MHD configuration close to a new equilibrium configuration with smaller total energy. A point can be reached where the field suddenly relaxes to the new equilibrium, if (sufficiently fast) fluid motions are allowed within the stably stratified NS interior.

As long as the early (ages much less than $\sim 10^4$ yr) evolution of magnetars is concerned, however, ambipolar diffusion in the NS core is expected to be the dominant mode of field decay.

Ambipolar diffusion drives a slow motion of charged particles with respect to background neutrons, which is opposed by both particle friction and chemical potential gradients in the stably stratified NS medium. GR92 identified two separate modes of ambipolar diffusion, differing by their effect on chemical composition. The solenoidal mode does not perturb chemical equilibrium and thus is counteracted only by particle friction. The irrotational mode, on the other hand, does perturb chemical equilibrium and cannot evolve on timescales shorter than the β-reaction timescale.

As shown in TD96, β-reactions are very efficient at erasing chemical equilibrium imbalance when $T > T_{\mathrm{tr}} \approx 5.73 \times 10^8\ (\rho_{15}/0.7)^{1/12}$ K. At these high temperatures, both modes of ambipolar diffusion are effectively opposed by neutron-proton friction only. Field decay occurs on the same timescale in both modes (GR92)

$$\begin{aligned}t_d^{(early)} &= \frac{4\pi n_e^2}{\lambda B^2}\left(\frac{L}{a}\right)^2 \simeq \\ &\simeq 2.2\times 10^4 \left(\frac{T}{10^9\mathrm{K}}\right)^2 \left(\frac{\rho_{15}}{0.7}\right)^{\frac{2}{3}} \left(\frac{B}{10^{16}\mathrm{G}}\right)^{-2} \mathrm{yr} \qquad (36)\end{aligned}$$

where L and a are the characteristic scale of variation of the Lorentz force and chemical potential, respectively, $(L/a) \approx 9.16\ T_9^4 \rho_{15}^{-1/3} (L/2\ \mathrm{km})$ (GR92). The latter is $\gg 1$ at high temperatures, given the high efficiency of β-reactions, while it becomes < 1 as the temperature drops and the efficiency of β-reactions decreases. At T$> 10^9$ K, the timescale (36) is much longer than the NS age or its cooling timescale. Therefore, field decay is negligible as long as the temperature is this high.

As NS cooling proceeds, the point is reached (at $T \leqslant T_{\mathrm{tr}}$) where chemical equilibrium imbalance becomes the main obstacle against which magnetic stresses must work to drive particle diffusion. This affects only the irrotational mode, while the solenoidal mode still decays on the timescale of eq. (36). Hence, the two modes grow at different rates with the irrotational mode evolving on a longer timescale[9] (TD96, GR92)

$$\begin{aligned}t_d^{(late)} &= \frac{4\pi n_e^2}{\lambda B^2} = \left(\frac{L}{a}\right)^{-2} t_d^{(early)} \approx \\ &\approx 7\times 10^3 \left(\frac{T}{T_{\mathrm{tr}}}\right)^{-6} \left(\frac{\rho_{15}}{0.7}\right)^{5/6} \left(\frac{L}{2\mathrm{km}}\right)^{\frac{3}{2}} \left(\frac{B}{10^{16}\mathrm{G}}\right)^{-2} \mathrm{yr} \qquad (37)\end{aligned}$$

TD96 considered in detail this lower-temperature regime. Based on stability arguments, these authors suggested that the solenoidal mode is expected to carry just a small fraction of the magnetic energy, most of it being tapped by the

[9] The two timescales are formally equal at $T = T_{\mathrm{tr}}$, but the irrotational mode becomes quickly much slower below $T = T_{\mathrm{tr}}$. For example, a 20% decrease of T below $T = T_{\mathrm{tr}}$ gives a 6 times longer decay timescale for the irrotational mode.

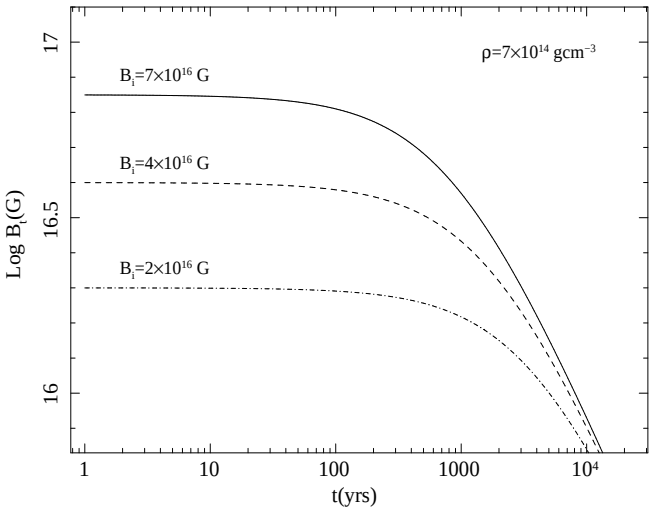

Figure 4. Expected evolution of the magnetic field intensity - at a specific value of the density $\rho = 7 \times 10^{14}$ g cm^{-3} $= 2.5\rho_{\rm nuc}$ - for three selected values of the initial intensity (B_i). Temperature equilibrium according to eq. (44) is assumed at each time. The tracks converge, as the field strength approaches $\approx 7 \times 10^{15}$ G, towards the asymptotic solution given by TD96.

irrotational mode. The main conclusion of this scenario is that only a tiny fraction of the magnetic energy reservoir in the NS core is lost either in the high-T regime, or via field decay through the solenoidal mode at lower temperatures. Most of the magnetic energy dissipation occurs via the slow decay of the irrotational mode, at $T \leqslant T_{\rm tr}$. This is based on the assumption that field decay, and the irrotational mode in particular, is effectively frozen at $T > T_{\rm tr}$.

The above scenario holds for fields in the 10^{15} G range. According to eq. (eq. 36), field decay at higher temperatures is significantly faster for stronger magnetic fields. Further, dissipation of even a small fraction of the magnetic energy reservoir may in principle affect NS cooling, if the reservoir is sufficiently large. In fact, field decay at T$> 10^9$ K is not frozen if B is larger than 10^{16} G. In analogy to the treatment of TD96, we check here whether an equilibrium condition between heating and cooling in the high-T regime can apply as well, with field decay described by eq. (36). For uniformity with that work we adopt the same normalizations for the parameters used by TD96.

We can write the heating rate per unit volume through field decay

$$\frac{dU^+}{dt} = \frac{B^2}{4\pi t_d^{(early)}} \approx 3.69 \times 10^{19} \ \frac{B_{16}^4}{T_9^2 \ \rho_{15}^{\frac{2}{3}}} \ \ {\rm erg\ cm^{-3} s^{-1}} \quad (38)$$

while the cooling rate per unit volume through modified Urca reactions is

$$\frac{dU^-}{dt} \simeq 9.6 \times 10^{20} \ T_9^8 \ \rho_{15}^{\frac{2}{3}} \ {\rm erg\ cm^{-3} s^{-1}} \quad . \quad (39)$$

Equating the two rates gives the equilibrium temperature

$$T_{\rm eq} \simeq 6.6 \times 10^8 \left(\frac{B}{10^{16}\ {\rm G}}\right)^{\frac{2}{5}} \left(\frac{\rho_{15}}{0.7}\right)^{-\frac{2}{15}} \left(\frac{L}{2{\rm Km}}\right)^{-\frac{1}{5}} \ {\rm K} \quad (40)$$

Note that $T_{\rm eq}$ is higher than $T_{\rm tr}$ if $B \geqslant 7 \times 10^{15}$ $(\rho_{15}/0.7)^{13/24}(L/2{\rm km})^{-1/8}$ G. Fields larger than that would thus be able to dissipate enough energy and balance neutrino cooling even in the early phase when the solenoidal and irrotational mode are still degenerate. This conclusion describes a regime that was not considered in Thompson & Duncan (1996): very strong magnetic fields ($\sim 10^{16}$ G) decaying and heating a NS core at very high temperatures ($\sim 10^9$ K) and at very young ages (years to centuries). The resulting evolution of magnetic field and temperature are coupled, as already shown by TD96. Our solution (eq. 40) joins smoothly the one found by TD96 (their eq. 31) in the sense that both give the same value of the magnetic field strength ($B \approx 7 \times 10^{15}$ G) when calculated at $T_{\rm tr}$. The two regimes are, in this sense, complementary, forming a continuous evolutionary sequence through $T_{\rm tr}$ for an arbitrarily large magnetic field whose decay is driven by ambipolar diffusion.

In order to better illustrate this, we calculate here the joint evolution of the magnetic field strength and the equilibrium temperature, according to the equilibrium conditions discussed above. Consider the rate of magnetic energy dissipation per unit volume

$$\frac{B}{4\pi}\frac{dB}{dt} = -\frac{B^2}{4\pi t_d^{(early)}} \quad , \quad (41)$$

Inserting eq. (36) and (40) in (41) gives

$$\frac{dB_{16}}{dt} \approx -3.12 \times 10^{-12} \left(\frac{\rho_{15}}{0.7}\right)^{-\frac{2}{5}} \ B_{16}^{\frac{11}{5}} \left(\frac{L}{2{\rm km}}\right)^{-\frac{8}{5}} \quad , \quad (42)$$

whose solution is

$$B_{16}(t) = \left[1.12 \times 10^{-4} \left(\frac{\rho_{15}}{0.7}\right)^{-\frac{2}{5}} \ \frac{t}{\rm yr} + \left(\frac{1}{B_{i,16}}\right)^{\frac{6}{5}}\right]^{-\frac{5}{6}} \quad (43)$$

with B_i the strength of the magnetic field at the initial time t_i. As an illustrative example, in Fig. 4 we show the evolution of the core magnetic field according to eq. (43), for three different initial values. The corresponding equilibrium temperature evolution is:

$$T_{8,eq} \simeq 6.6 \left[1.1 \times 10^{-4} \frac{t}{\rm yr} \left(\frac{\rho_{15}}{0.7}\right)^{-\frac{2}{5}} + \left(\frac{1}{B_{i,16}}\right)^{\frac{6}{5}}\right]^{-\frac{1}{3}} \quad (44)$$

We caution that the equilibrium temperature as a function of density is in principle different from the actual temperature profile throughout the NS core. Finding this would require solving the heat flux problem self-consistently, which includes account for the strong suppression of heat transport across magnetic field lines in a superstrong magnetic field.

With the above expressions for the equilibrium regime, the decay timescales of the two modes of ambipolar diffusion can be evaluated self-consistently - given an initial magnetic core field $B_{t,i}$ - and their values compared. In Fig. 5 we show, for illustration, the evolution of the two timescales for an initial (uniform) core magnetic field $B_{t,i} = 5 \times 10^{16}$ G and at a given value of the density $\rho_{15} = 0.7$. Clearly, field evolution is always determined by the longest decay time: as long as particle friction dominates, both modes decay on the timescale $t_d^{(early)}$. Once chemical equilibrium imbalance overtakes particle friction (at $t \approx 10^4$ yrs in our example), the two modes split: the solenoidal mode is unaffected and continues to evolve on the (now shorter) time $t_d^{(early)}$, while the irrotational mode is now subject to a slower evolution,

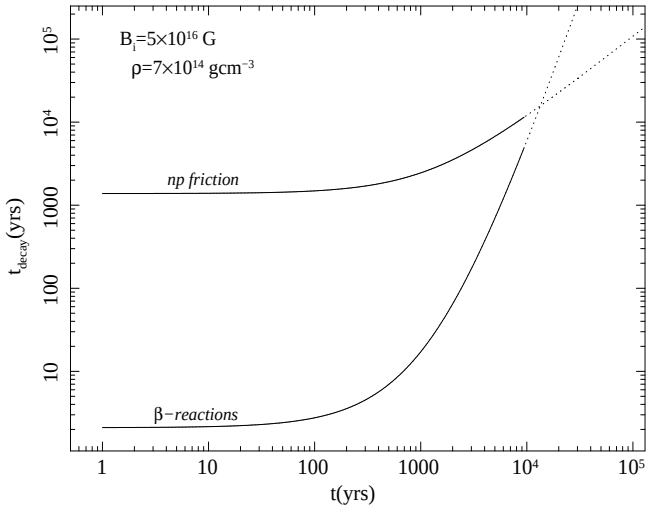

Figure 5. Evolution of the ambipolar diffusion decay timescales determined by each of the two friction mechanisms, separately, calculated at a particular density $\rho = 2.5\rho_{\rm nuc}$ and for a given initial field strength $B_i = 5 \times 10^{16}$ G. The timescales evolve according to their dependence on the temperature T and magnetic field B. The evolution of T(t) and B(t) is given by eqs. (44) and (43) and is thus determined by *np*-friction alone, initially. However, the β-reaction timescale is a much stronger function of time than the *np*-friction timescale, in this regime. Curves are dotted where the two timescales become comparable, within a factor of a few, and the approximation under which timescales are calculated - through eqs. (43) and (44) - does not hold anymore. At this point, the temperature is close to the transition temperature $T_{\rm tr}$ and the magnetic field close to the value $\approx 7 \times 10^{15}$ G (see text).

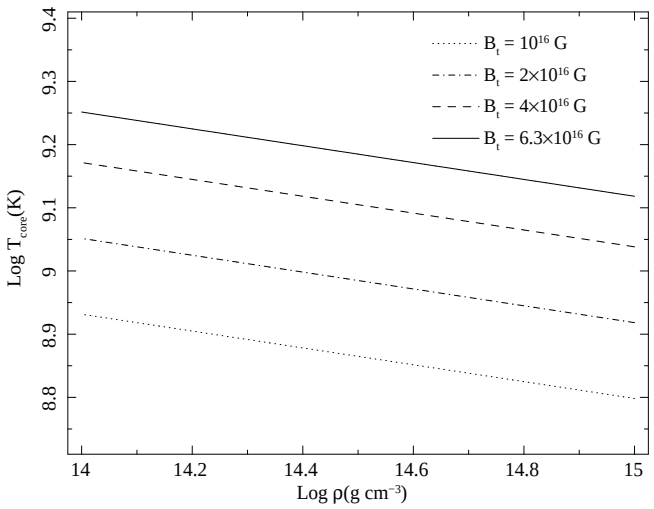

Figure 6. Value of the equilibrium temperature (eq. 44) as a function of density throughout the NS core, for four selected values of the magnetic field strength, as indicated in the figure.

determined by the efficiency of β-reactions.
We show in Fig. 4 the evolution of the core magnetic field in the regime described here, for three different initial values. More details are given in the captions.

We can also estimate the time Δt after which the temperature, once equilibrium between heating and cooling holds, reaches the transition value[10] $T_{\rm tr}$

$$\frac{\Delta t}{\rm yr} \approx 1.36 \times 10^4 \left(\frac{\rho_{15}}{0.7}\right)^{-\frac{1}{4}} \left(\frac{L}{2{\rm km}}\right)^{\frac{7}{4}} \times \times \left[1 - 0.657 \left(\frac{1}{B_{i,16}}\right)^{\frac{6}{5}} \left(\frac{\rho_{15}}{0.7}\right)^{-\frac{8}{5}} \left(\frac{L}{2{\rm km}}\right)^{\frac{32}{35}}\right] \quad (45)$$

This gives $\Delta t \sim 4500$ yrs for $B_i = 10^{16}$ G and has an asymptotic value $(\Delta t)_{\rm max} \simeq 1.36 \times 10^4$ yrs for very large B. For $B_i = 3{\times}10^{16}$ G, $\Delta t \simeq 1.1{\times}10^4$ yrs, $\sim 80\%$ of the asymptotic value. The comparison with a NS standard cooling scenario, without any heat sources, is striking, since in this case $T_{\rm tr}$ is reached in somewhat less than 10 yrs.
Once the field has decayed to the limiting value $\simeq 7 \times 10^{15}$ G, the temperature equals $T_{\rm tr}$ and the results obtained by TD96 hold. We conclude that the early thermal evolution of the core can be significantly altered (slowed down) by ultra-strong field decay. A detailed analysis of the consequences of this conclusion is beyond our scope here and will be the subject of future study.

5.1 Comparison with recent studies of core heating in magnetars

Surface temperatures inferred from the X-ray spectra of SGRs/AXPs (> 0.35 keV, or $> 4 \times 10^6$ K) are a factor $\sim 2 \div 3$ higher than expected from cooling calculations of NSs with their estimated ages, $\sim 10^4$ yrs (Kaminker et al. 2007). The heat source internal to the NS needs thus not only be strong enough to provide the excess energy but it also needs to be efficiently converted to *surface* heating.

Kaminker et al. (2007) considered how the surface temperature of a cooling NS would be affected when a (slowly decaying) heating source in its interior were included, in order to account for the heating provided by the decaying magnetic field. These authors suggest that, if heat is released in the core or deep crustal layers, only a minor fraction of it is transported to the surface and radiated thereby as X-ray photons. Rahter, most of the released heat produces an enhancement in neutrino emission - which is strongly temperature dependent - and is thus radiated locally (via neutrinos). In fact, in their calculations the local temperature in the core is affected only slightly by internal heating. Core temperatures never reach 10^9 K and the surface can't ever be kept as warm as AXPs/SGRs surface emission indicates. Kaminker et al. (2007) conclude that heat is most likely released in the outer regions of the crust, where neutrino-emitting processes are much less efficient and heat is thus most efficiently transported to the surface, with only minor losses.

Their results are therefore at variance with ours, that envisage an efficient heating of the core up to very high temperatures (as a function of the magnetic field strength). The difference bewteen the two conclusions is readily found in the parametrization of the heating source chosen by

[10] This time is zero by definition for $B_i = 7 \times 10^{15}$ G

Kaminker et al. (2007), which corresponds to a different physical scenario.

Their model heat source is independent on the magnetic field strength and on the NS internal temperature. The maximum initial heating rate they consider ($Q_0 = 3 \times 10^{20}$ erg/s) effectively corresponds to our expression (38) with $B \simeq 1.6 \times 10^{16}$ G. The heating rate in their model decreases exponentially in time, with a fixed time constant comparable to, but somewhat longer than, the source estimated age. As opposed to this, we have *i*) allowed for initially stronger fields and, thus, larger heating rates and *ii*) considered a time-varying decay timescale, since the ambipolar diffusion-driven field decay is a function of the NS internal temperature and field strength (eq. 38). In particular, the values of T and B at each epoch are determined self-consistently by the equilibrium condition between cooling and heating.

As a consequence, in the model by Kaminker et al. (2007) the released heat does not affect the value of Q while it enhances neutrino emission. The latter being a strong function of the temperature, the net result is a slight enhancement of the interior temperature, to make neutrinos able to carry away almost all the eccess heat.

In ambipolar-diffusion driven field decay, on the other hand, heating has a feedback on both cooling *and* heating itself. As long as the temperature is very high the NS cools, with heating providing just a minor perturbation to the dominant process of ν-cooling. As the core temperature drops, however, the field decay rate grows (eq. 38) while neutrino emission drops. Eventually, the two rates become almost equal and at this stage their equilibration plays a key role, as stressed by TD96. Near equilibrium, temperature variations have a strong feedback on both heating and cooling - and with opposite effects. This forces the temperature toward T_{eq} (eq. 40): as the field dissipates the temperature drops slighlty and a new equilibrium between heating and cooling is reached, at a slightly smaller temperature and field strength. The equilibrium temperature within the NS core, as a function of density, obtained through our eq. (40) is shown in Fig. (6) for four different values of the average core magnetic field strength. In Fig. (7) we show, for a given initial magnetic field strength, the equilibrium temperature throughout the magnetar core at four different epochs of its evolution according to eq. (41). More details are given in the caption.

Therefore, the internal heating source considered by Kaminker et al. (2007) differs from ambipolar diffusion-driven field decay. When ambipolar diffusion in the core - and the associated heating - is taken into account, the NS core can remain at fairly high temperatures for a long time *if the decaying field is around* $\sim 10^{16}$ *G.*

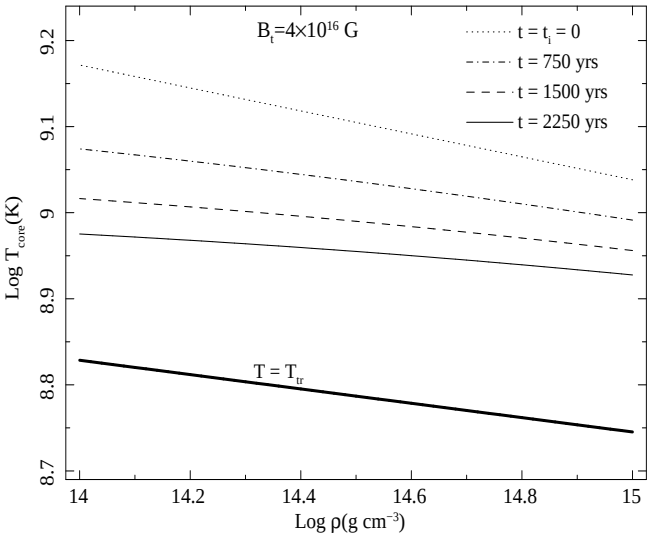

Figure 7. The evolution of the temperature profile within a magnetar core (10^{14} g cm$^{-3} < \rho \leqslant 10^{15}$ g cm^{-3}) for a specific initial value of the toroidal field strength ($B_t = 4 \times 10^{16}$ G), corresponding to a total magnetic energy $E_B \simeq 4.6 \times 10^{50}$ erg or an ellipticity $\epsilon_B \approx -4.6 \times 10^{-3}$. The four curves describe the temperature profile at four different epochs, the thick solid curve at the bottom defines the temperature at (and below) which chemical equilibrium imbalance becomes the major limiting factor for ambipolar diffusion of the irrotational mode (the regime described in TD96). Above the thick line, the irrotational and solenoidal mode are degenerate and the regime described in the previous section holds.

6 CONCLUSIONS

In this paper we have investigated some implications of one of the key ansatz of the magnetar model; namely, that magnetars do form with millisecond spin periods and a (mainly) toroidal magnetic field, generated through the strong differential rotation of the collapsing proto-neutron star (DT92 and TD93).

Building on our earlier work (Stella et al. 2005, Dall'Osso & Stella 2007), we showed that one major implication of this scenario is that such objects can become strong sources of GWs in the first few days after formation. This results *if* there exists at least a tiny misalignment (angle χ) between the rotation axis and the symmetry axis of the magnetic field, at birth. The newly born NS is distorted to a prolate shape by the toroidal field, and is freely precessing because of $\chi \neq 0$. Under these circumstances internal viscous dissipation of the precessional motion will drive the magnetic symmetry axis orthogonal to the spin axis, the most favourable geometry for GW emission.

We discussed current uncertainties in various aspects of the model and introduced simple approximations to treat each of them. We developed a simple analytical model describing the early rotational evolution of newly formed magnetars, that includes an ideal magnetic dipole torque plus the GW torque acting on an orthogonal, prolate rotator (see eq. 4). We then estimated the magnitude of GW emission from magnetars s as a function of their initial spin, internal magnetic energy and external (dipole) magnetic field (as well as their mass and radius).

Our main conclusions can summarized as follows:

- if magnetars are born with spin period less than 3 ms, internal toroidal fields $\geqslant 3 \times 10^{16}$ G and external dipole fields $\leqslant 2 \times 10^{14}$ G then the expected GW signal would be strong enough to be detectable with Advanced LIGO/Virgo class detectors out to the Virgo cluster, where their formation rate may be ~ 1 per year;
- the estimated optimal S/N ratios for match-filtered signal searches (with one detector only) are very encouraging.

However, as already noted by Stella et al. (2005), optimal signal searches have unaffordable computational costs. The developement of sub-optimal signal search strategies is required, a task that is currently under way.

• if our scenario holds, the rotational energy $\simeq 3\times10^{52}$ $(\mathrm{P/ms})^2$ ergs of the newly formed magnetar will be emitted mostly as GWs, in the first few days after formation. As a consequence, Supernova Remnants (SNRs) surrounding evolved magnetars would not be expected to bear the signature of an excess energy injection ($> 10^{51}$ erg) soon after formation, since GWs do not interact appreciably with the expanding shell.

In particular, the condition that a newly formed magnetar be detectable as a GW source from Virgo-cluster distances turns out to be almost equivalent to the condition that it radiate less than 10^{51} erg through magnetic dipole radiation. The two requirements are met for nearly overlapping regions of the internal and external magnetic fields parameter space. Stated differently, if the Galactic magnetar candidates studied by Vink & Kuiper (2006) were born with millisecond spin periods, $\mathrm{B}_t > 3\times10^{16}$ G and $\mathrm{B}_d \leqslant 2\times10^{14}$, they would have lost most of their rotational energy through GW emission. Their SNRs would thus not show any excess energy compared to other SNRs - as observed, indeed - *and* the GW signal they emitted could have been detected out to ~ 20 Mpc with Advanced LIGO/Virgo class interferometers.

Finally, we considered the evolution of an internal field $> 10^{16}$ G as a result of ambipolar diffusion, as already envisaged by GR92 and TD96. Our aim here was twofold: first, we investigate this high B-field regime, for which the calculations by TD96 are not appropriate. Second, we showed that even fields this strong have (at least) a slow decay mode through ambipolar diffusion, that is active soon after formation. This process can prevent the cooling of the magnetar core below a temperature of $\sim 10^9$ K for hundreds to thousands years. This conclusion is expected to have significant implications for our understanding of AXPs/SGRs.

APPENDIX A: SPIN ENERGY AND FREEBODY PRECESSION ENERGY OF A ROTATING ELLIPSOID

We give here a quick derivation of the expression for the energy of freebody precession of a fluid star subject to both centrifugal and magnetic deformations. A more general discussion, in the context of "ordinary" NSs, is found in Jones & Andersson (2001).

First of all, we write down the frequency of the freebody precession mode derived by Mestel & Takhar (1972)

$$\omega_{\rm pre} = \frac{I_3 - I_1}{I_1}\Omega\cos\psi = \epsilon_B\Omega\cos\psi \quad , \tag{A1}$$

where angles throughout this section are those defined in Fig. A1.

Following Jones & Andersson 2001 (and references therein), we define the moment of inertia tensor of the fluid NS as a linear combination of three contributions, namely a (spherical) gravitational part, plus two axisimmetric perturbations provided, in our case, by the centrifugal and magnetic fields, respectively. Hence:

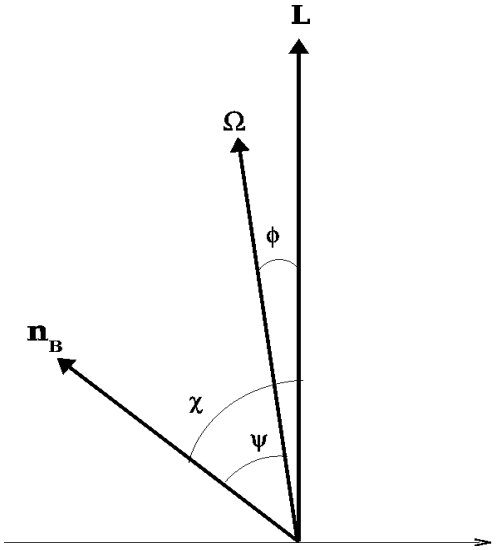

Figure A1. Schematic representation of the angles of interest to the problem. L represents the invariant angular momentum vector, Ω is the angular frequency vector and n_B is represents the unit vector along the simmetry axis of the magnetic field. The angle $\phi \simeq \epsilon_B \sin\psi\cos\psi \ll \psi$ (Jones & Andersson 2001). Therefore, $\psi \approx \chi$.

$$\underline{\boldsymbol{I}} = I_0\underline{\boldsymbol{\delta}} + \Delta I_\Omega(\hat{\boldsymbol{n}}_\Omega\hat{\boldsymbol{n}}_\Omega - \underline{\boldsymbol{\delta}}/3) + \Delta I_B(\hat{\boldsymbol{n}}_B\hat{\boldsymbol{n}}_B - \underline{\boldsymbol{\delta}}/3) \tag{A2}$$

where $\underline{\boldsymbol{\delta}}$ is the identity, $\hat{\boldsymbol{n}}_{\Omega,B}$ represent the unit vectors along the spin and magnetic field axis and $\Delta I_{\Omega,B}$ are the magnitudes of the corresponding perturbations of the inertia tensor. The eigenvalues of the latter are (Jones & Andersson 2001):

$$\begin{aligned}
\mathrm{I}_1 &= \mathrm{I}_0 + \frac{2}{3}\Delta\mathrm{I}_\Omega - \frac{1}{3}\Delta\mathrm{I}_B \\
\mathrm{I}_2 &= \mathrm{I}_0 + \frac{2}{3}\Delta\mathrm{I}_\Omega - \frac{1}{3}\Delta\mathrm{I}_B \\
\mathrm{I}_3 &= \mathrm{I}_0 + \frac{2}{3}\Delta\mathrm{I}_\Omega + \frac{2}{3}\Delta\mathrm{I}_B = \mathrm{I}_1 + \Delta\mathrm{I}_B
\end{aligned} \tag{A3}$$

These expressions show that the centrifugal deformation modifies all eigenvalues in the same way, as if it was effectively a spherically symmetric, additive term. The magnetic deformation, on the other hand, does introduce an asimmetry between the first two eigenvalues and the third one, inducing the magnetic ellipticity $\epsilon_B \equiv (\mathrm{I}_3 - \mathrm{I}_1)/\mathrm{I}_1$. The angle ϕ between $\boldsymbol{\Omega}$ and the angular momentum axis is always smaller than the tilt angle χ of the magnetic symmetry axis (Jones & Andersson 2001). In formulae, to first order in ϵ_B it can be shown that (by using eq. A2)

$$\sin\phi \approx \phi \simeq \epsilon_B\ \sin\psi\cos\psi \ll \psi \quad , \tag{A4}$$

from which $\psi = \chi - \phi \simeq \chi$.

Following the argument by Cutler & Jones (2001), the NS angular momentum can be written as $\boldsymbol{L} = \underline{\boldsymbol{I}}\boldsymbol{\Omega}$ and its kinetic energy as $\mathrm{E_k} = (1/2)\underline{\boldsymbol{I}}\boldsymbol{\Omega}\cdot\boldsymbol{\Omega}$, from which (to first order in ϵ_B)

$$\begin{aligned}
\mathrm{L} &= \mathrm{I}_1\Omega\left(1 + 2\epsilon_B\cos^2\psi\right)^{1/2} \simeq \mathrm{I}_1\Omega\left(1 + 2\epsilon_B\cos^2\chi\right)^{1/2} \\
\mathrm{E_k} &= \frac{1}{2}\mathrm{I}_1\Omega^2(1 + \epsilon_B\cos^2\psi) \simeq \frac{1}{2}\mathrm{I}_1\Omega^2(1 + \epsilon_B\cos^2\chi).
\end{aligned} \tag{A5}$$

From the latter equation we can obtain the energy of freebody precession by taking the difference between the second equation in (A5) and the spin energy of the same ellipsoid that, with the same total angular momentum $\boldsymbol{L}$, spins around the axis having the greatest moment of inertia. The latter configuration is indeed the one that minimizes the energy, at constant angular momentum. It is thus the one towards which a freely precessing spheroid will evolve, given an internal dissipative process (Mestel & Takhar 1972; Jones 1976; Cutler 2002). Therefore, if Ω is the angular frequency of the precessing spheroid and $\Omega_{\rm F}$ the angular frequency once freebody precession is completely damped, conservation of angular momentum implies

$$\left(\frac{\Omega_{\rm F}}{\Omega}\right)^2 = \left(\frac{I_1}{I_{\rm max}}\right)^2 \left(1+2\epsilon_B \cos^2\chi\right). \quad \text{(A6)}$$

Writing the minimum spin energy as $\mathrm{E_{min}} = \frac{1}{2}\mathrm{I_{max}}\Omega_{\rm F}^2$, the freebody precession energy is

$$\begin{aligned} \mathrm{E_{prec}} &= \mathrm{E_k} - \frac{1}{2}\mathrm{I_{max}}\Omega_{\rm F}^2 \\ &= \frac{1}{2}\mathrm{I_1}\Omega^2\left\{1+\epsilon_B\cos^2\chi - \frac{\mathrm{I_1}}{\mathrm{I_{max}}}\left(1+2\epsilon_B\right)\right\}. \end{aligned} \quad \text{(A7)}$$

This general expression can be specialized to the case of an oblate ($\mathrm{I_{max}} = \mathrm{I_3}$) or a prolate ($\mathrm{I_{max}} = \mathrm{I_1} = \mathrm{I_2}$) ellipsoid giving[11], respectively

$$\begin{aligned} \mathrm{E_{prec}} &\simeq \frac{1}{2}\mathrm{I_1}\Omega^2\epsilon_B \sin^2\chi \quad \text{oblate ellipsoid } (\epsilon_B>0) \\ \mathrm{E_{prec}} &\simeq -\frac{1}{2}\mathrm{I_1}\Omega^2\epsilon_B \cos^2\chi \quad \text{prolate ellipsoid } (\epsilon_B<0). \end{aligned} \quad \text{(A8)}$$

to first order in ϵ_B.
Self consistence of the above is warranted by $\mathrm{E_{prec}} \to 0$ for $\chi \to 0$ in the oblate case, and for $\chi \to \pi/2$ in the prolate case.
From the above formulae we can eventually relate the time derivative of the freebody precession energy to the time derivative of the tilt angle χ, in the case of a prolate ellipsoid. Since conservation of angular momentum is required, Ω changes only as a consequence of changes in χ (cfr. eq. A6), which makes the time derivative of $\mathrm{E_{prec}}$ a function of $\dot{\chi}$ only. Taking the time derivatives of the first of eq. (A5) and the second of eq. (A8) and requiring angular momentum conservation we obtain (to first order in ϵ_B)

$$\frac{\mathrm{dE_{prec}}}{\mathrm{dt}} \simeq \mathrm{I_1}\epsilon_B\Omega^2\dot{\chi}\cos\chi\sin\chi = -2\mathrm{E_{prec}}\tau_{\rm d}^{\chi} \quad \text{(A9)}$$

where $\tau_{\rm d}^{\chi}$ was defined in § 2.1.4.

APPENDIX B: CALCULATION OF THE DAMPING TIME OF FREEBODY PRECESSION THROUGH BULK VISCOSITY

In this appendix we describe the calculation that leads to the estimated timescale for dissipation of the free precessional motion through bulk viscosity (eq. 13). According to the definition of $\tau_{\rm d}$ (eq. 12), we need an expression for both the bulk viscosity coefficient, ζ, and the precession-induced density perturbation, $\delta\rho$.

[11] Note that the precession energy is positive in both cases, as it *must* be

For the bulk viscosity coefficient, we recall here the general expression (11)

$$\mathrm{Re}(\zeta) = \frac{n\tau\left(\partial p/\partial x\right)_n d\tilde{x}/dn}{1+(\omega\tau)^2} \simeq \frac{n\left(\partial p/\partial x\right)_n d\tilde{x}/dn}{\omega^2\tau}. \quad \text{(B1)}$$

For *npe* matter, as we have assumed throughout, the timescale for β-reactions (τ_β) is (cfr. Reisenegger & Goldreich 1992)

$$\tau_\beta = \frac{3n_p}{\lambda_\beta E_{F_n}} \simeq \frac{0.23}{T_9^6}\left(\frac{\rho}{\rho_{\rm nuc}}\right)^{\frac{2}{3}} \ \text{yr}. \quad \text{(B2)}$$

Here $\tilde{x}$ is the equilibrium fraction of charged particles (see below), $E_{F_n} = (h^2/2m_n)(3\pi^2 n_n)^{2/3}$ is the neutron Fermi energy and $\lambda_\beta \simeq 5\times10^{33}T_9^6(\rho/\rho_{\rm nuc})^{2/3}$ erg^{-1} s^{-1} is the rate of β-reactions when the combined fluid is out of chemical equilibrium by an amount $\delta\mu = \delta\mu_n - \delta\mu_e - \delta\mu_p$. Finally, $\rho_{\rm nuc} \approx 2.8\times10^{14}$ g cm^{-3} is the nuclear saturation density. The last step in eq. (11) holds for $\omega_{\rm pre}\tau_\beta \gg 1$, the relevant approximation here.
The pressure of degenerate *npe* matter, neglecting the small contribution from protons, is given by $p \simeq \frac{2}{5}m_nE_{F_n} + \frac{1}{4}m_eE_{F_e}$ where the equilibrium proton (and electron) fraction is (Reisenegger & Goldreich 1992)

$$\tilde{x} = \left(\frac{n_p}{n_n}\right)_{\rm eq} \approx \frac{n_p}{n} \simeq 6\times10^{-3}\frac{\rho}{\rho_{\rm nuc}}. \quad \text{(B3)}$$

From all the above, one obtains the required expression (cfr. Sawyer 989):

$$\begin{aligned} \zeta &\approx 6\times10^{-59}\frac{\rho^2T^6}{\omega_{\rm pre}^2} \approx \\ &\approx \frac{5.6\times10^{29}}{\cos^2\chi}\left(\frac{\rho_{15}}{0.7}\right)^2\left(\frac{\mathrm{P}}{\mathrm{ms}}\right)^2\left(\frac{10^{50}\mathrm{erg}}{\mathrm{E_B}}\right)^2 T_{10}^6\frac{\mathrm{erg}}{\mathrm{cm}} \end{aligned} \quad \text{(B4)}$$

As a starting poin to determine the density perturbation $\delta\rho$, we refer to the expression given by Mestel & Takhar (1972) of the centrifugal distortion of a fluid star, ρ_Ω, as a function of a spherical coordinate system whose origin is at the star center and whose pole is the magnetic pole (r,θ,λ) .
The amplitude of internal field of motion, ξ, is determined by the non-spherical part of the rotational distortion of the fluid. The perturbation of the density profile is

$$\delta\rho_\Omega = \rho_\Omega(\lambda-\Omega t) - \rho_\Omega(\lambda) = \frac{1}{2}f(r)\hat{K}(\chi,\theta,\lambda,\Omega t) \ . \quad \text{(B5)}$$

where the function $\hat{K}(\chi,\theta,\lambda,\Omega)$ is

$$\begin{aligned} \hat{K}(\chi,\theta,\lambda,\Omega) &= \sin^2\chi[1-P_2(\mu)]\times \\ &\times \{\sin2\lambda\,\sin2\Omega t - \cos2\lambda(1-\cos2\Omega t)\} + \\ &+ 3\,\sin\chi\cos\chi\sin2\theta\,[\sin\lambda\,\sin\Omega t - \\ &- \cos\lambda(1-\cos\Omega t)] \ . \end{aligned} \quad \text{(B6)}$$

Here, $P_2(\mu) = P_2(\cos\theta)$ is the Legendre polynomial. The radial function $f(r)$, that depends on the stellar model assumed, can only be obtained analytically through approximate (and/or idealized) calculations.
In particular, the centrifugal deformation of a fluid mass with a polytropic equation of state is an old problem that has been largely discussed in the literature. We refer, here, to the study by Chandrasekhar (1933), where both analytical formulae and numerical values for the relevant functions are derived.

Given the polytropic EOS $p = k\rho^{1+1/n}$, one can define an adimensional density variable

$$\rho = \rho_c \left(\frac{\rho}{\rho_c}\right)^n = \rho_c \Theta^n \ . \quad \text{(B7)}$$

The ratio of the rotation energy to the gravitational binding energy defines the rotation parameter v

$$v = \frac{\Omega^2}{2\pi \mathrm{G}\rho_c} \ . \quad \text{(B8)}$$

in powers of which the adimensional density Θ can be expanded. In the above G is the gravitational constant and ρ_c the central density of the fluid star. For $v \ll 1$, a first order expansion will suffice. Introducing the adimensional radial coordinate ξ, such that $r = \alpha\xi$, the first order expansion of the density profile becomes

$$\Theta(\xi) = \theta_0(\xi) + v\psi(\xi) \ , \quad \text{(B9)}$$

where θ_0 is the unperturbed density profile, solution to the Lane-Emden equation for a non-rotating polytrope. The parameter α above is related to the polytropic equation of state

$$\alpha = \left[\frac{(n+1)\ k}{4\pi G}\ \rho_c^{-1+1/n}\right]^{1/2} \stackrel{(n=1)}{\rightarrow} \left(\frac{k}{2\pi \mathrm{G}}\right)^{1/2} \ . \quad \text{(B10)}$$

The problem is thus reduced to finding an appropriate expression for the function $\psi(\xi)$. In particular, for polytropes of index n the following expansion holds

$$\Theta(\xi) = \theta_0 + v\left[\psi_0(\xi) + A_2\psi_2(\xi)P_2(\mu)\right] \ , \quad \text{(B11)}$$

where $\psi_0(\xi)$ is the spherical part of the centrifugal deformation and the non-spherical part of the deformation corresponds to the second term in square parenthesis. The coefficient A_2 is

$$A_2 = -\frac{5}{6}\frac{\xi_R^2}{3\psi_2(\xi_R) + \xi_R\psi_2'(\xi_R)} \ , \quad \text{(B12)}$$

where $\alpha\xi_R = R$ and the prime denotes a first derivative. An approximate analytical expression for $\psi_2(\xi)$ is given as an eighth-order polynomial expansion in ξ (Chandrasekhar 1933)

$$\psi_2(\xi) = \xi^2 - \frac{1}{14}\xi^4 + \frac{1}{504}\xi^6 - \frac{1}{33264}\xi^8 + o(\xi^{10}) \ , \quad \text{(B13)}$$

which formally completes the problem at hand.

As it has been shown by numerical integration of the equilibrium equations, a first-order expansion in v provides a relatively good approximation to slowly rotating polytropes; in the case $n = 1$, $v \leqslant 0.075$ gives approximately the rotation rate at which deviations from the first order perturbation theory become non-negligible (Tassoul 1978). In particular, direct integration of the equilibrium equations reveals a systematically larger deformation of rapid rotators compared to the results obtained through the first order perturbative approximation. Therefore, our general expectation would be that the latter underestimates the real deformation of a rapidly rotating NS ($\delta\rho$), thus underestimating the efficiency of bulk viscous dissipation.

The polytropic index $n = 1$ greatly simplifies the analytical treatment and allows one to derive quite straightforward formulae. The adimensional radius of the polytropic star will be $\xi_R = \pi$ and the numerical values of $\psi_2(\xi_R)$ and $\psi_2'(\xi_R)$ have been tabulated by Chandrasekhar (1933), allowing to derive $A_2(n = 1) \simeq -0.54833$. Finally, α is determined by the linear scale for the NS radius so that:

$$\alpha \simeq 3.82 \times 10^5 \left(\frac{\mathrm{R}}{12\ \mathrm{Km}}\right) \ \mathrm{cm} \quad \text{(B14)}$$

and the EOS thus becomes $p = 6.1146 \times 10^4\ (\mathrm{R}/12\ \mathrm{Km})^2\ \rho^2$. The density perturbation of eq. (B5), the one that determines the precession-induced internal motions damped by bulk viscosity, amounts to only the non-spherical part of the centrifugal deformation. The spherical part does not cause any radial periodic motions and, thus, does not perturb the local chemical potential equilibrium of NS matter. We are therefore left with:

$$f(r(\xi)) = \rho_c v A_2 \psi_2(\xi) \quad \text{(B15)}$$

where the angular part corresponds to the function $K(\chi, \theta, \lambda, \Omega)$. This must be inserted in eq. (B5) to obtain the full expression for the non-spherical density perturbation. Recalling eq. (12), we thus get the full expression for the bulk viscosity damping rate:

$$\dot{\mathrm{E}}_{\mathrm{diss}} = 60 T_{10}^6\ \omega^2 \int \mathrm{dV} \left(\frac{\delta\rho}{\rho}\right)^2 \frac{\rho^2}{\omega^2} = 60 T_{10}^6 \int \mathrm{dV} (\delta\rho)^2 \quad \text{(B16)}$$

where:

$$\begin{aligned} [\delta\rho(r(\xi))]^2 &= \frac{1}{4} f^2(r(\xi)) K^2(\chi, \theta, \lambda, \Omega) = \\ &= \frac{1}{4}(\rho_c v)^2 A_2^2 \psi_2^2(\xi) \hat{K}^2(\chi, \theta, \lambda, \Omega) \end{aligned} \quad \text{(B17)}$$

so that, eventually, the full expression for $\dot{\mathrm{E}}_{\mathrm{diss}}$ can be written as:

$$\begin{aligned} \dot{\mathrm{E}}_{\mathrm{diss}} &\approx 2.6 \times 10^{13} T_{10}^6 \Omega^4 \alpha^3 \int \psi_2^2(\xi)\xi^2 \mathrm{d}\xi \int \hat{K}^2\ \sin\theta \mathrm{d}\theta \mathrm{d}\lambda \\ &\approx 2.2 \times 10^{45} \left(\frac{\mathrm{T}}{10^{10}\mathrm{K}}\right)^6 \left(\frac{\mathrm{ms}}{\mathrm{P}}\right)^4 \left(\frac{\mathrm{R}}{12\mathrm{Km}}\right)^3 \times \\ &\times \int \psi_2^2(\xi)\xi^2 \mathrm{d}\xi \int \hat{K}^2 \sin\theta \mathrm{d}\theta \mathrm{d}\lambda \end{aligned} \quad \text{(B18)}$$

The radial integral, solved from $\xi = 0$ to $\xi_R = \pi$ gives 138.04, while the angular part gives $(24\pi/5)\sin^2\chi(1+3\cos^2\chi)$. Eventually:

$$\begin{aligned} \dot{\mathrm{E}}_{\mathrm{diss}} &\approx 4.7 \times 10^{48}\ \sin^2\chi(1 + 3\cos^2\chi) \\ &\left(\frac{\mathrm{T}}{10^{10}\mathrm{K}}\right)^6 \left(\frac{\mathrm{ms}}{\mathrm{P}}\right)^4 \left(\frac{\mathrm{R}}{12\mathrm{Km}}\right)^3 \mathrm{erg\ s^{-1}} \end{aligned} \quad \text{(B19)}$$

As a last step, given the energy of the freebody precession mode derived in § A, we obtain the dissipation timescale (see eq. 13):

$$\begin{aligned} \tau_{\mathrm{d}} = \frac{2E_{\mathrm{pre}}}{\dot{\mathrm{E}}_{\mathrm{diss}}} &\simeq \frac{13.5\ \cos^2\chi}{\sin^2\chi(1 + 3\cos^2\chi)} \left(\frac{\mathrm{E}_B}{10^{50}\mathrm{erg}}\right)^2 \left(\frac{\mathrm{P}}{\mathrm{ms}}\right)^2 \\ &\times \left(\frac{\mathrm{T}}{10^{10}\mathrm{K}}\right)^{-6} \left(\frac{\mathrm{M}}{1.4\mathrm{M}_\odot}\right) \left(\frac{\mathrm{R}}{12\mathrm{Km}}\right)^3 \mathrm{s} \end{aligned} \quad \text{(B20)}$$

ACKNOWLEDGMENTS

This work was supported by Virgo-EGO Scientific Forum (VESF) Fellowship at the University of Pisa.

S.D. acknowledges N. Andersson for suggesting to check for the possible role of bulk viscosity in damping freebody precession of a newly formed NS.

As one of the thousands Italian researchers with medium-term positions, SD acknowledges the support of Nature (455, 835-836) and thanks the Editors for increasing the international awareness of the current critical situation of Italian Research and of young researchers *in primis*.

REFERENCES

Abbott, B., et al., 2007, PRD, 76, 042001
Allen, M. P., & Horvath, J. E. 2004, Ap.J., 616, 346
Alpar, M. A., & Sauls, J. A., 1988, Ap.J., 327, 723
Arons, J., 2003, Ap.J. 589, 871
Arras, P., Cumming, A., & Thompson, C., 2004, Ap.J.L., 608, L49
Blandford, R. D., Applegate, J. H., & Hernquist, L., 1983, M.N.R.A.S., 204, 1025
Blandford, R. D., & Romani, R. W., 1988, M.N.R.A.S., 234, 57P
Bonazzola, S., & Gourgoulhon, E. 1996, Astr. & Astroph., 312, 675
Bucciantini, N., Thompson, T. A., Arons, J., Quataert, E., & Del Zanna, L., 2006, M.N.R.A.S., 368, 1717
Bucciantini, N., Quataert, E., Arons, J., Metzger, B. D., & Thompson, T. A., 2007, M.N.R.A.S., 380, 1541
Camilo, F., Kaspi, V. M., Lyne, A. G., Manchester, R. N., Bell, J. F., D'Amico, N., McKay,N. P. F., & Crawford, F., 2000, Ap.J., 541, 367
Chandrasekhar, S. 1933, M.N.R.A.S., 93, 390
Contopoulos, I., Kazanas, D., & Fendt, C., 1999, Ap.J., 511, 351
Contopoulos, I., & Spitkovsky, A., 2006, Ap.J., 643, 1139
Cumming, A., Arras, P., & Zweibel, E., 2004, Ap.J., 609, 999
Cutler, C., & Jones, D. I., 2001, PRD, 63, 024002
Cutler, C., 2002, PRD, 66, 084025
Dall'Osso, S., Israel, G. L., Stella, L., Possenti, A., & Perozzi, E., 2003, Ap.J., 599, 485
Dall'Osso, S., & Stella, L., 2007, Astroph. & Space Science, 308, 119
Dib, R., Kaspi, V. M., & Gavriil, F. P., 2008, Ap.J., 673, 1044
Duncan, R. C. 1998, Ap.J.L., 498, L45
Duncan, R. C., & Thompson, C. 1992, Ap.J.L., 392, L9
Ferrario, L., & Wickramasinghe, D. 2006, M.N.R.A.S., 367, 1323
Gaensler, B. M., Gotthelf, E. V., & Vasisht, G., 1999, Ap.J.L., 526, L37
Geppert, U., & Rheinhardt, M., 2006, Astr. & Astroph., 456, 639
Goldreich, P., 1970, Ap.J.L., 160, L11
Goldreich, P., & Reisenegger, A. 1992, Ap.J., 395, 250
Gruzinov, A., 2006, arXiv:astro-ph/0604364
Haskell, B., Samuelsson, L., Glampedakis, K., & Andersson, N., 2008, M.N.R.A.S., 385, 531
Ioka, K., 2001, M.N.R.A.S., 327, 639
Israel, G. L., Götz, D., Zane, S., Dall'Osso, S., Rea, N., & Stella, L., 2007, Astr. & Astroph., 476, L9
Jones, P. B. 1976, Astrophysics and Space Science, 45, 369
Jones, D. I., & Andersson, N., 2001, M.N.R.A.S., 324, 811
Kaminker, A. D., Yakovlev, D. G., Potekhin, A. Y., Shibazaki, N., Shternin, P. S., & Gnedin, O. Y., 2007, Astroph. & Space Science, 308, 423
Lattimer, J. M., & Prakash, M. 2001, Ap.J., 550, 426
Lattimer, J. M., & Prakash, M., 2007, Phys. Rep., 442, 109
Lazzati, D., Ghirlanda, G., & Ghisellini, G., 2005, M.N.R.A.S., 362, L8
Lindblom, L., Owen, B. J., & Morsink, S. M., 1998, Phys. Rev. Lett., 80, 4843
Lindblom, L., Mendell, G., & Owen, B. J., 1999, PRD, 60, 064006
Lindblom, L., & Owen, B. J. 2002, PRD, 65, 063006
Link, B., Epstein, R. I., & Baym, G., 1992, Ap.J.L., 390, L21
Livingstone, M. A., Kaspi, V. M., Gavriil, F. P., Manchester, R. N., Gotthelf, E. V. G., & Kuiper, L., 2007, Astroph. & Space Science, 308, 317
Losurdo G., 2007, "Advanced Virgo sensitivity curve: cavity finesse and signal recycling tuning", Virgo Internal Report: VIR024A07
Lyne, A. G., Pritchard, R. S., & Smith, F. G., 1988, M.N.R.A.S., 233, 667
Lyne, A. G., Pritchard, R. S., Graham-Smith, F., & Camilo, F., 1996, Nature, 381, 497
Lyutikov, M., 2003, M.N.R.A.S., 346, 540
Marshall, F. E., Gotthelf, E. V., Middleditch, J., Wang, Q. D., & Zhang, W., 2004, Ap.J., 603, 682
Mazets, E. P., Golentskii, S. V., Ilinskii, V. N., Aptekar, R. L., & Guryan, I. A. 1979, Nature, 282, 587
Mereghetti, S., & Stella, L., 1995, Ap.J.L., 442, L17
Mestel, L., & Takhar, H. S. 1972, M.N.R.A.S., 156, 419
Metzger, B. D., Thompson, T. A., & Quataert, E., 2007, Ap.J., 659, 561
Middleditch, J., Marshall, F. E., Wang, Q. D., Gotthelf, E. V., & Zhang, W., 2006, Ap.J., 652, 1531
Nakar, E., Gal-Yam, A., Piran, T., & Fox, D. B., 2006, Ap.J., 640, 849
Ostriker, J. P., & Gunn, J. E. 1969, Ap.J., 157, 1395
Owen, B. J., Lindblom, L., Cutler, C., Schutz, B. F., Vecchio, A., & Andersson, N., 1998, PRD, 58, 084020
Owen, B. J., & Lindblom, L., 2002, Classical and Quantum Gravity, 19, 1247
Paczynski, B., 1992, Acta Astronomica, 42, 145
Page, D., Lattimer, J. M., Prakash, M., & Steiner, A. W. 2004, Ap.J. Suppl., 155, 623
Page, D., Geppert, U., & Weber, F., 2006, Nuclear Physics A, 777, 497
Palomba, C., 2001, Astr. & Astroph., 367, 525
Pons, J. A., & Geppert, U., 2007, Astr. & Astroph, 470, 303
Pons, J. A., Link, B., Miralles, J. A., & Geppert, U., 2007, Phys. Rev. Lett., 98, 071101
Popov, S. B., & Stern, B. E., 2006, M.N.R.A.S., 365, 885
Reisenegger, A., & Goldreich, P. 1992, Ap.J., 395, 240
Ruderman, M., 1991, Ap.J., 366, 261
Ruderman, M., Zhu, T., & Chen, K., 1998, Ap.J., 492, 267
Sawyer, R. F., 1989, PRD, 39, 3804
Spitkovsky, A., 2006, Ap.J.L., 648, L51
Stella, L., Dall'Osso, S., Israel, G. L., & Vecchio, A., 2005, Ap.J.L., 634, L165
Tanvir, N. R., Chapman, R., Levan, A. J., & Priddey, R. S., 2005, Nature, 438, 991
Tassoul, J. L., 1978, Theory of Rotating Stars, Princeton

University Press, Princeton University, New Jersey
Thompson, T. A., Chang, P., & Quataert, E., 2004, Ap.J., 611, 380
Thompson, C., & Duncan, R. C. 1993, Ap.J., 408, 194
Thompson, C., & Duncan, R. C. 1995, M.N.R.A.S., 275, 255
Thompson, C., & Duncan, R. C. 1996, Ap.J., 473, 322
Thompson, C., & Duncan, R. C. 2001, Ap.J., 561, 980 5
Ushomirsky, G., Cutler, C., & Bildsten, L. 2000, M.N.R.A.S., 319, 902
Usov, V. V., 1992, Nature, 357, 472
Vink, J., & Kuiper, L. 2006, M.N.R.A.S., 370, L14
Woods, P. M., & Thompson, C., 2006, Compact stellar X-ray sources, 547

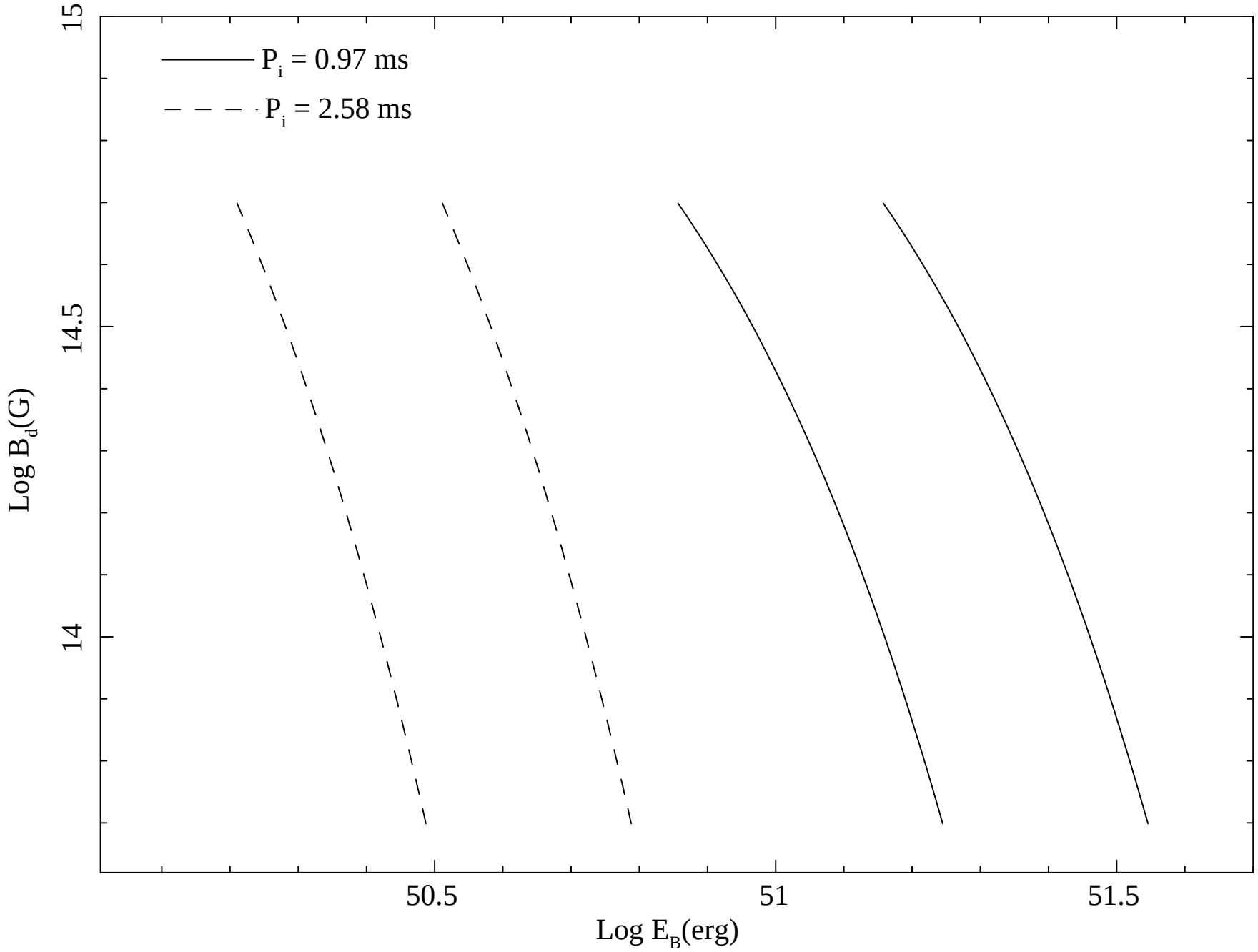
P_i = 0.97 ms
P_i = 2.58 ms
15
14.5
14
Log B_d(G)
50.5
51
51.5
Log E_B(erg)